

Argonne National Laboratory  
9700 South Cass Avenue  
Argonne, Illinois 60439

**HIGH ENERGY PHYSICS DIVISION  
SEMIANNUAL REPORT OF  
RESEARCH ACTIVITIES**

*January 1, 1999 - June 30, 1999*

Prepared from information gathered and edited by  
the committee for Publications and Information:

Members: J. Norem  
R. Rezmer  
C. Schuur  
R. Wagner

January 2000

## Table of Contents

I.	<b>Experimental Research Program</b> .....	1
	A. Experiments With Data.....	1
	1. Medium Energy Physics Program .....	1
	2. Collider Detector at Fermilab .....	2
	a) Physics Results .....	2
	b) Run II Planning .....	7
	3. Non-Accelerator Physics at Soudan .....	8
	a) Physics Results .....	8
	b) Experimental Apparatus, Operation and Maintenance .....	11
	c) Planning Activities .....	11
	4. ZEUS Detector at HERA.....	11
	a) Physics Results .....	11
	b) HERA and ZEUS Operations.....	19
	B. Experiments In Planning Or Construction.....	19
	1. MINOS-Main Injector Neutrino Oscillation Search.....	19
	2. ATLAS Detector Research & Development .....	21
	a) Overview of ANL ATLAS Tile Calorimeter Activities .....	21
	C. Detector Development .....	22
	1. The CDF Upgrade Project .....	22
	2. ZEUS Detector Upgrade.....	24
	a) Straw Tube Tracker Readout Electronics.....	24
	3. ATLAS Calorimeter Design and Construction .....	25
	a) Calorimeter Construction .....	25
	b) Calorimeter Instrumentation and Testing .....	30
	c) Test Beam Program .....	30
	d) Extended Barrel QC Program.....	31
	4. MINOS Detector Development .....	34
	5. Electronics Support Group .....	36
II.	<b>Theoretical Physics Program</b> .....	39
	A. Theory.....	39
	1. Single Top-Squark Production Via R-Parity-Violating Super-symmetric Couplings in Hadron Collisions .....	39
	2. Resummation of Large Corrections to Heavy-Quarkonium Decays .....	42
	3. NLO QCD Predictions for SUSY Particle, Jet, and Lepton Pair Production.....	43
	4. Computational Physics.....	43
	5. Phase-Space Quantization of Field Theory .....	46

III.	<b>Accelerator Research And Development</b> .....	48
	A.    Argonne Wakefield Accelerator Program .....	48
	1.    Facility Status/Upgrade Plans. ....	48
	2.    Experimental Program.....	50
	a)    11.4 GHz Structure.....	50
	b)    Multimode Structure Wakefields .....	51
	c)    Slab Symmetric Laser Driven Accelerators .....	52
	B.    MUON Collider R & D .....	54
	1.    Lithium Lens Design.....	54
IV.	<b>Divisional Computing Activities</b> .....	56
	A.    Grand Challenge Applications.....	56
	1.    Data Access for High-Energy and Nuclear Physics R&D .....	56
V.	<b>Publications</b> .....	57
	A.    Journal Publications, Conference Proceedings, Books .....	57
	B.    Papers Submitted for Publication .....	62
	C.    Papers or Abstracts Contributed to Conferences .....	64
	D.    Technical Reports and Notes .....	68
VI.	<b>Colloquia and Conference Talks</b> .....	73
VII.	<b>High Energy Physics Community Activities</b> .....	78
VIII.	<b>High Energy Physics Division Research Personnel</b> .....	81

# I. EXPERIMENTAL RESEARCH PROGRAM

## I.A. EXPERIMENTS WITH DATA

### I.A.1 Medium Energy Physics Program

In the period January - June, 1999 accomplishments for the ANL-HEP division medium energy physics project consisted of the completion of two papers on past Saclay experiments, the beginning of analysis of recent data from the Crystal Ball measurements at the Brookhaven AGS, and preparations for a RHIC polarimeter.

Two papers on Saclay pp elastic scattering data were completed by an ANL physicist, submitted and accepted in Physical Review,. Results for the spin observable  $P = A_{\text{ooon}} = A_{\text{ooon}} = A_y$  at over 30 beam kinetic energies between 800 and 2800 MeV and c.m. angles from about  $70^\circ - 110^\circ$  are described. A total of 919 new data points are presented in these articles. The energy dependence at fixed c.m. angles appears smooth, with no evidence for rapid energy-dependent structure. Work has also begun on two additional papers at Argonne and on others at Saclay.

Measurements of reactions with  $\pi^-$ ,  $K^-$ , and  $\bar{p}$  beams on a liquid hydrogen target to all neutral final states were made with the Crystal Ball detector at the Brookhaven AGS in late 1998. Analysis has begun at Argonne and Valparaiso University on some of the kaon and antiproton beam data. The  $\bar{p}p \rightarrow \text{neutrals}$  reactions are being studied event-by-event using a special display program and calculations of invariant masses of sets of detected energy clusters. In addition, the  $K^-p \rightarrow \Sigma^0\pi^0 \rightarrow (\gamma n\pi^0)\pi^0$  reaction has been identified in the data, and improved cuts are being studied. Finally, many additional counters and materials are being added to the Monte Carlo simulation program for the experiment. These additions will permit a more accurate evaluation of corrections to the integrated pion or kaon beam striking the target.

A paper related to some of the Crystal Ball studies was also published in this period. The experiment was run at Los Alamos, and the article is titled "Analyzing Power for the  $\pi^- \bar{p} \rightarrow \pi^0 n$  Reaction Across the  $\Delta(1232)$  Resonance," Phys. Rev. **C60**, 024604 (1999).

With the completion of polarization experiment E-925 at the AGS, the preliminary data have demonstrated that inclusive charged pion production can be used for a high-energy polarimeter. There are plans for some of the E-925 counters and cables to be used for such a polarimeter at RHIC, and some preparatory work was begun during this period. In addition, a part of the E-925 equipment was removed from the experiment and packed for shipment to Argonne.

(H. Spinka)

## I.A.2 Collider Detector at Fermilab

### a. Physics Results

In B physics, the multiple tag CP analysis of  $B^0/\bar{B}^0 \rightarrow \Psi K_s^0$ , with Barry Wicklund providing oversight as B physics convener and Larry Nodulman appointed as chief internal reviewer, became public for the later winter conferences. The result,  $\sin(2\beta) = 0.79^{+0.41}_{-0.44}$ , illustrated by the asymmetry plotted in Figure 1, represents a substantial improvement over our earlier same side tag measurement. It tends to support the expected large positive CP violating asymmetry as shown in unitarity triangle plot of Figure 2. A draft article for publication has been made ready to present to the collaboration. Karen Byrum continues efficiency studies for a cross section measurement, which are used by the Toronto group in  $b$  jet fragmentation results.

An example of one of the many tasks Barry has taken on as B physics convener is working with the Texas Tech group to show that a purported exclusive  $B_c$  signal was not robust. Larry Nodulman was involved in oversight of settling 94-95 data luminosity issues, which as resolved left some unresolved issues in  $\psi$  reconstruction efficiency as a function of instantaneous luminosity. Barry convinced the proponents to avoid these relatively small effects by extrapolating to zero luminosity. The  $\psi$  and  $Y$  cross sections and angular distributions are quite interesting QCD topics, without requiring cross section precision at the level of the  $\pm 4\%$  luminosity uncertainty.

In electroweak physics, a comprehensive  $W$  mass analysis was put together and made public for the winter conferences. The energy scale discrepancy between E/p calibration and the  $Z$  mass has not been resolved, and since some mysteries remain in tracking, despite considerable improvements, we decided to use the  $Z$  mass to set the scale for both electron and muon measurements. These scales, as well as resolutions, are illustrated in Figure 3. The electron fit is illustrated in Figure 4. The combined electron and muon result for the 94-95 data is  $80.470 \pm 0.089$ , which combined with earlier CDF measurements gives  $80.433 \pm 0.079$  GeV/ $c^2$ . Of individual experiments, only D0 and ALEPH are comparable so far, but the LEP results continue to improve. The current world average is  $80.394 \pm 0.042$  GeV/ $c^2$ ; the direct  $W$  and top mass measurements are not yet as constraining as the  $Z$  pole measurements at LEP and SLC, as illustrated in Figure 5. An article on the  $W$  mass measurements is being prepared.

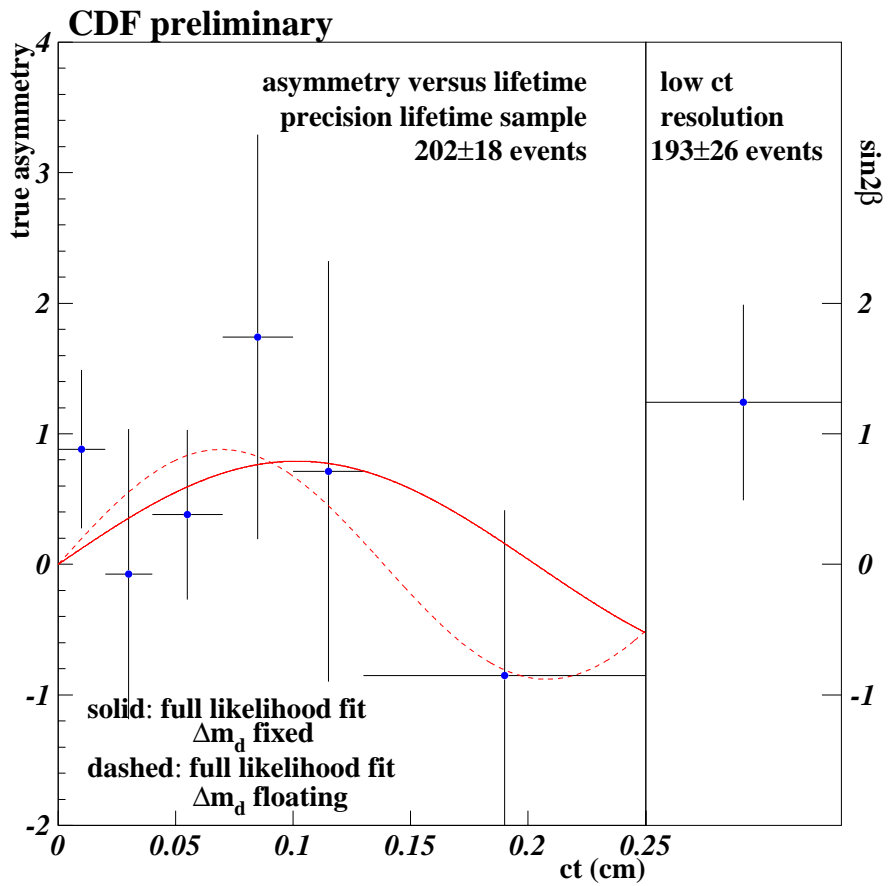


**Figure 1.** Dilution normalized CP asymmetry, left for the SVX sample as a function of proper time, and right integrated for the non-SVX sample.

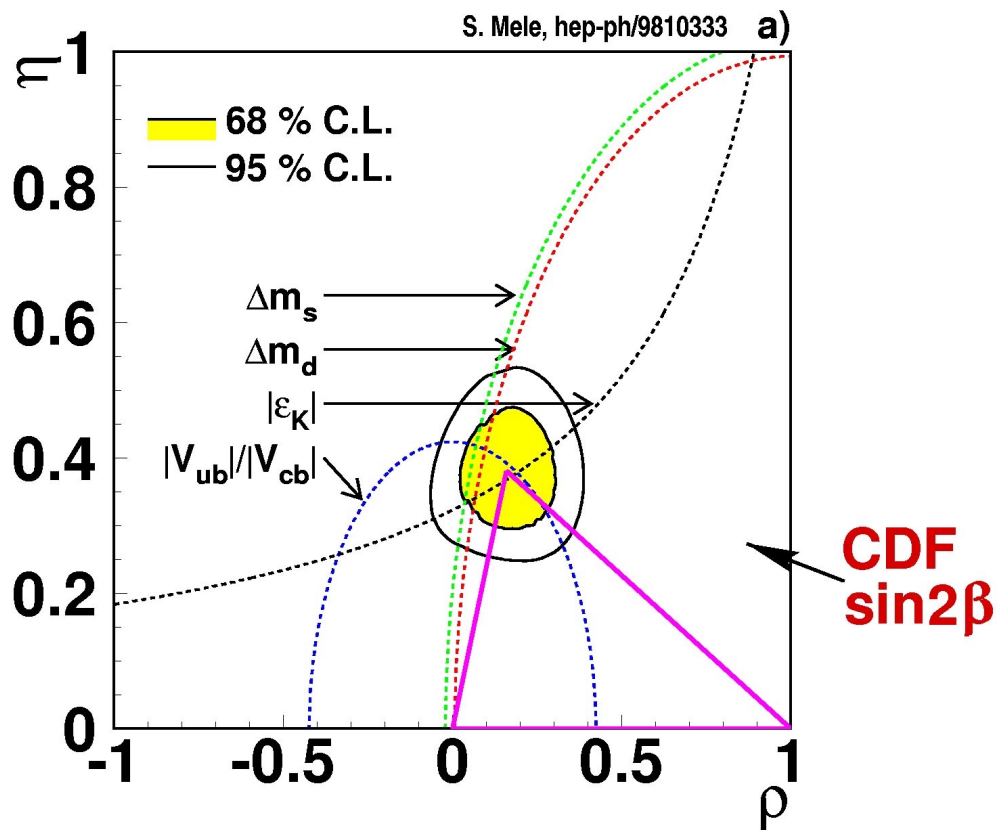


**Figure 2.** The CKM unitarity triangle: The curves show the central value contours for various measurements with the blob representing contours for an overall fit. Our direct measurement gives two (dashed) solutions and the solid 68% lines.

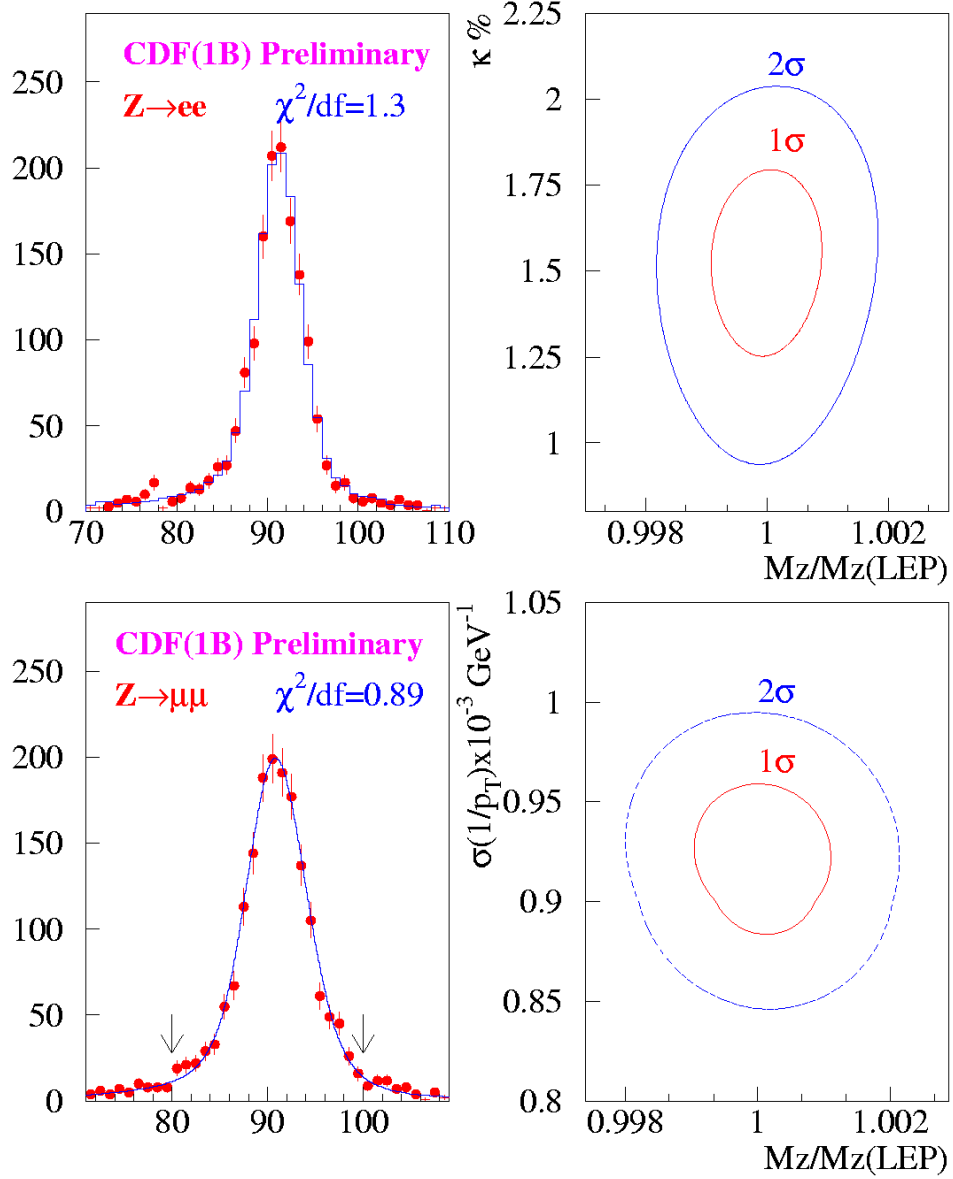


**Figure 3.** Lineshapes for electron and muon pair  $Z$  bosons, and the scale and resolution parameter contours derived from fitting the mass and width. For electrons, the parameter  $k$  is defined by  $\sigma(E) = \sqrt{(13.5\% \times \sqrt{E_T})^2 + k^2}$ ,  $E_T$  in GeV.

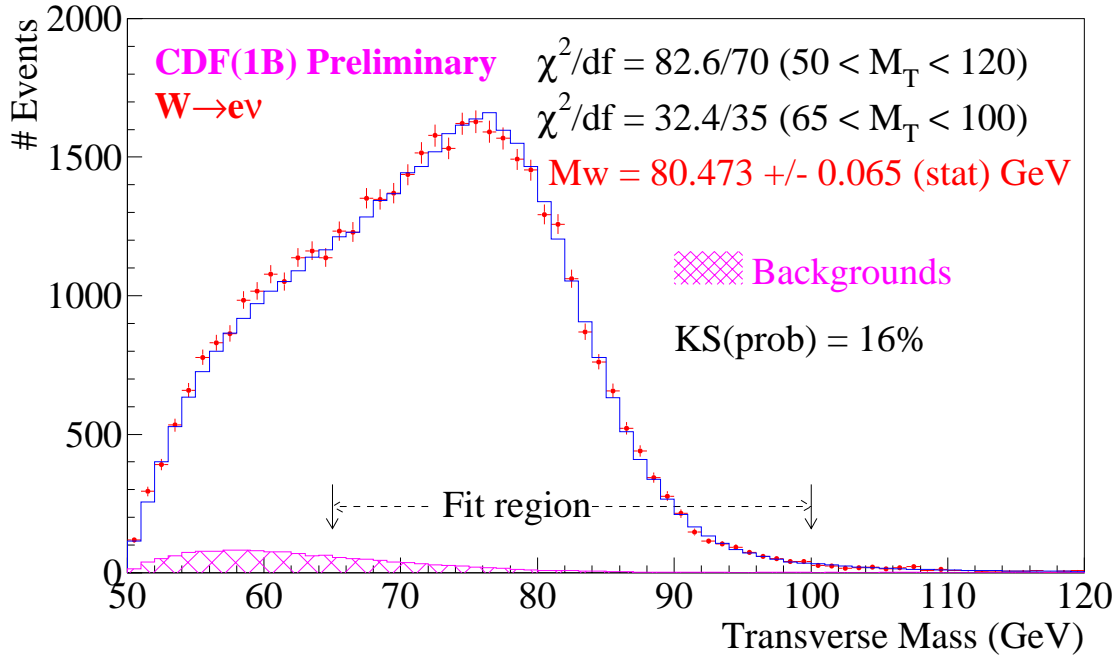


**Figure 4.** Transverse mass lineshape for electron  $W$  bosons, data, simulation, and background.

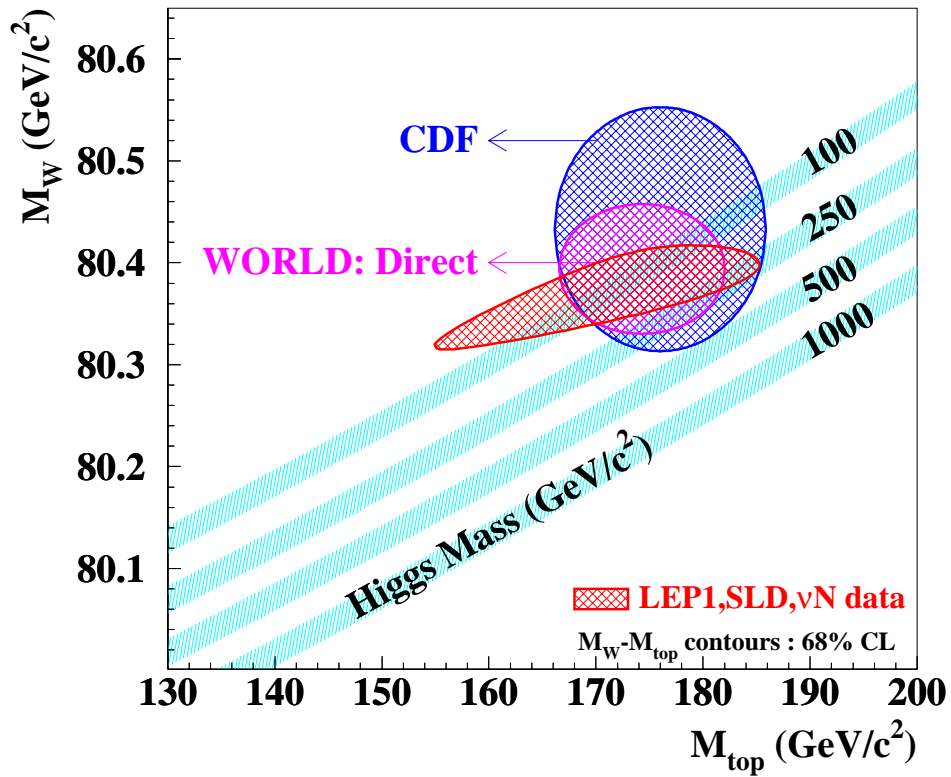


**Figure 5.** Indirect precision electroweak and direct measurement of the top and  $W$  masses showing Higgs mass contours.

In QCD studies, Steve Kuhlmann is working with the Brandeis group on inclusive direct photon production in the 94-95 data. The result has been approved and is shown in Figure 6. While this result is being prepared for publication, attention has turned to the  $\sqrt{s} = 630$  GeV data.

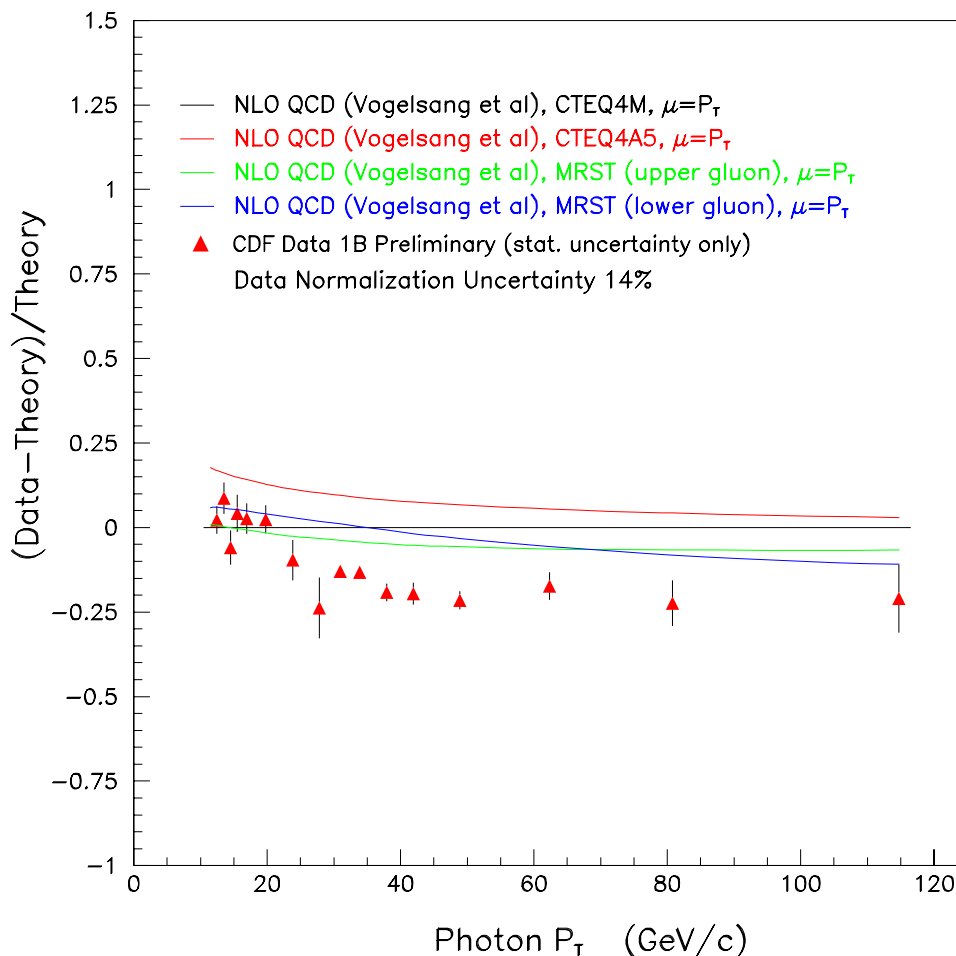


**Figure 6.** Theory normalized differential cross section for isolated photons from the 94-95 CDF data.

### b. Run II Planning

A series of Run II physics workshops continues at Fermilab. Steve Kuhlmann has taken a leading role in QCD issues and optimizing two  $b$  jet mass resolution for Higgs searches. Larry Nodulman has been involved in electroweak sessions. A new workshop on Tevatron Collider  $b$  physics is being organized for CDF, D0 and BTeV, and Barry Wicklund is one of the principal organizers. Barry also continues to take an important role within CDF in defining planned triggers and datasets for  $b$  physics.

(L. Nodulman)

### **I.A.3 Non-Accelerator Physics at Soudan**

#### **a. Physics Results**

The Soudan~2 detector continues to operate and analysis of contained events and muons continues to shed new light on the atmospheric neutrino anomaly and the search for nucleon decay. In addition, a long term study of atmospheric muons is now possible through almost a complete solar cycle. The cosmic ray shadows of the moon and sun test both the angular resolution and pointing of a cosmic ray detector. The angular diameter of both bodies as observed at the earth is  $0.5^\circ$ .

Observation of a shadow places limits on detector angular resolution and pointing accuracy, as well as on phenomena affecting cosmic ray propagation and interaction. These latter effects include deflections due to the geomagnetic field and, in the case of the sun, the solar and interplanetary magnetic fields, and smearing due to multiple Coulomb scattering and production mechanisms for air showers and muons.

Muon tracks in Soudan are reconstructed using two different software algorithms. If both algorithms provide satisfactory reconstructions, the directionality from the algorithm that provides the best angular resolution is used. The total reconstructed event data sample passing cuts consisted of  $3.4 \times 10^7$  muon events.

The time of each event is recorded using a time base synchronized to the WWVB time standard. The event time and the known detector coordinates specify the apparent direction of the moon, including the correction for parallax. The angle  $\theta$  between each muon track and the directions of the moon at the time of the event is then calculated. Figure 1 shows a plot of the angular density of muons,  $(1/\pi)(dN_\mu/d\theta^2)$  vs.  $\theta$ , the angular distance between the muon direction and the calculated position of the center of the moon. In the absence of a moon shadow, this plot should be flat, because the varying direction of the moon averages over any anisotropies in detector acceptance or rock overburden. The plot, however, clearly shows a deficit of events at small angles, which we attribute to a lunar cosmic ray shadow.

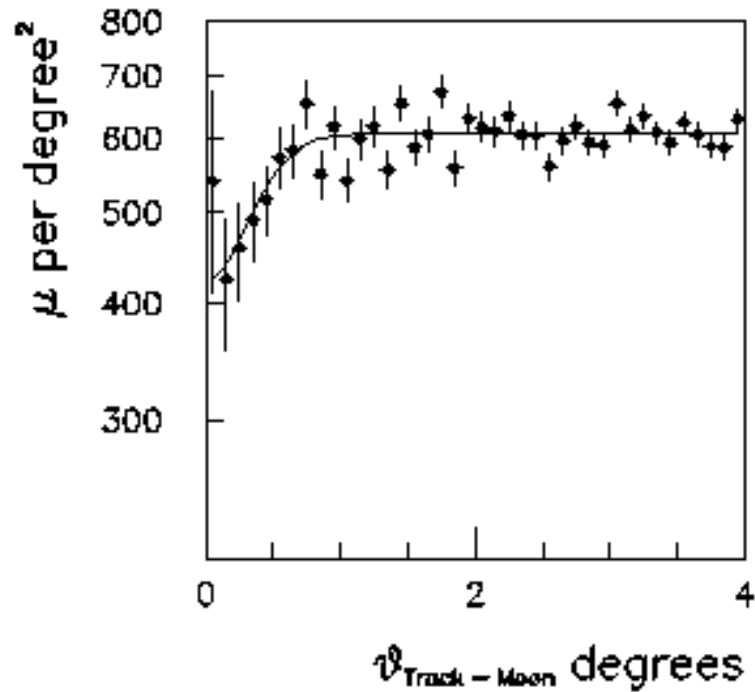


**Figure 1.** The angular distance between muons and the center of the moon.

To test the alignment and angular resolution of the Soudan 2 detector, we have constructed a two-dimensional contour map of the muon flux from the direction of the moon. This map, shown in Figure 2, was made using the normalized statistic  $Z_{i,j} = (d_{i,j} - b_{i,j}) / \sqrt{\text{var}(b_{i,j})}$  where  $d_{i,j}$  are the bin contents in the smoothed observed event histogram and  $b_{i,j}$  are the bin contents in the smoothed expected event histogram. Figure 2 suggests neither evidence for any misalignment of the Soudan 2 detector nor any indication of a shadow offset due to the geomagnetic field at the level of  $0.1^\circ$ . A comparison of the data collected during 1989 to 1994 and during 1995 through 1998 confirms that the detector alignment has remained stable over the entire data collection decade.

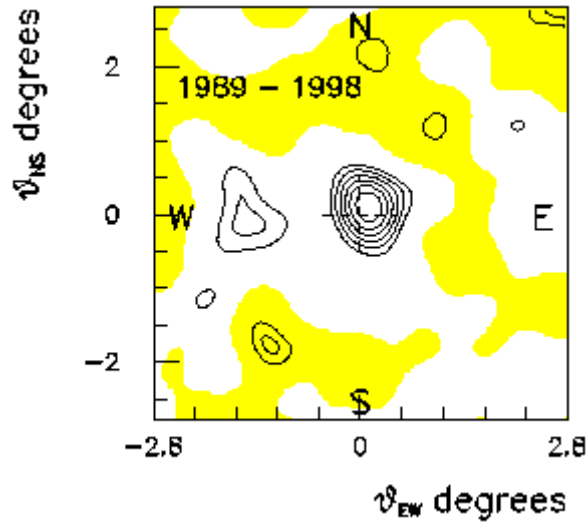


**Figure 2.** Contour map of the normalized deviations,  $Z$ , for a  $\pm 2.8^\circ \times \pm 2.8^\circ$  region centered on the moon with a rebinning kernel  $0.29^\circ$ .

The data from the sun is shown in Figure 3. The deficit is both shallower and wider than the moon shadow observed during the same interval, as is expected because of the effect of the interplanetary magnetic field. The 10-year collection interval spans much of an 11-year solar cycle during which solar magnetic field and sunspot activity peaked in 1989-1991 and was at a minimum level in 1996. If the data is divided in half, the shadow is clearly seen in the data from 1995 to 1998, a period of low field and sunspot activity. But there is no evidence for a distinct shadow in the 1989 to 1994 data. The average daily satellite-measured IPMF (sunspot number) was 4.8 nT(28) for the former interval and 6.7nT(104) for the latter one.

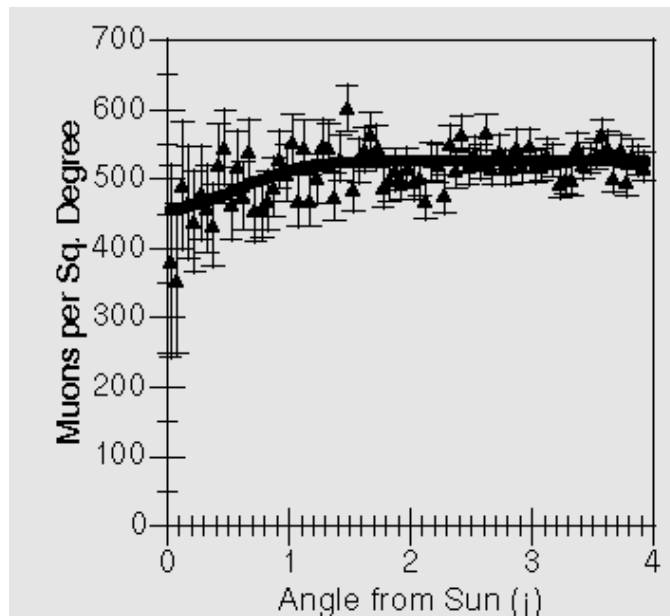


**Figure 3.** The angular distance between muons and the center of the sun.

## **b. Experimental Apparatus, Operation and Maintenance**

Argonne physicists continued to make substantial contributions to the maintenance and operation of the detector. Major activities included ongoing improvements of detector and electronics performance. Argonne physicists also continued the development of software to make use of  $dE/dx$  information from the detector.

## **c. Planning Activities**

The Soudan group plans to run the detector for nucleon decay, atmospheric neutrino and other cosmic ray studies until an exposure of 5.0 kt-year fiducial volume is achieved. After that, the Soudan detector will become an integral part of the MINOS long-baseline neutrino oscillation experiment. The progress on that project is described elsewhere in this report.

(M.C. Goodman)

## **I.A.4 ZEUS Detector at HERA**

### **a. Physics Results**

Six papers were published in this period and five more manuscripts were submitted for publication.

#### *i) ZEUS Results on the Measurement and Phenomenology of $F_2$ at Low $x$ and $Q^2$*

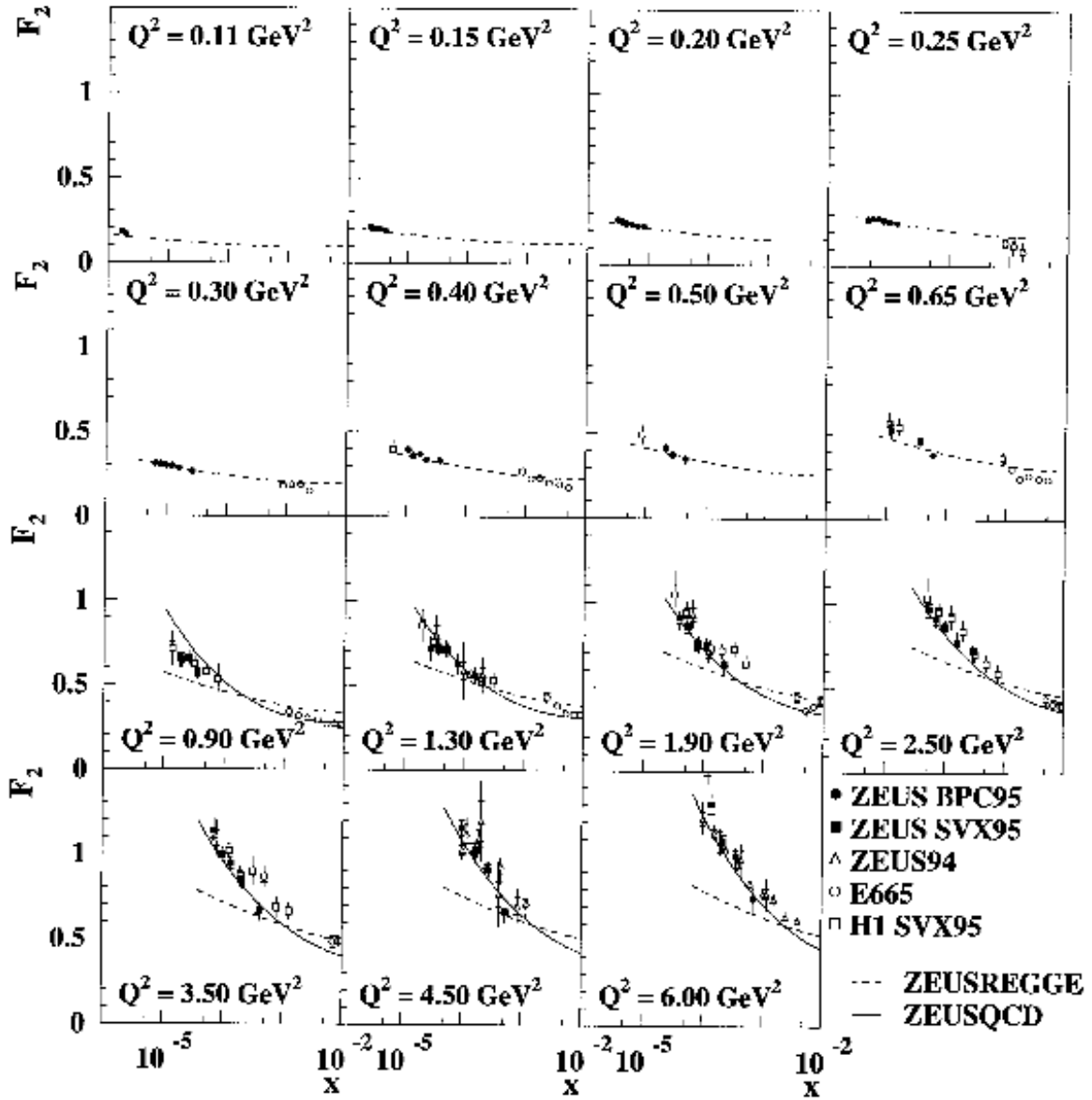
The rapid rise of the proton structure function  $F_2$  at low  $x$  continues to generate a lot of interest. In particular, the persistence of the strong rise to small values of  $Q^2$  and the apparent success of the perturbative QCD description of data down to  $Q^2$  values approaching 1  $\text{GeV}^2$  raise new challenges for our understanding of QCD. This paper is dedicated to the study of the ‘transition region’ as  $Q^2 \rightarrow 0$  in which pQCD must break down. Figure 1 shows a compilation of measurements of  $F_2$  in the region of  $Q^2$  between 0.11 and 6.0  $\text{GeV}^2$ , as obtained from measurements with the beam pipe calorimeter and with shifted vertex data, among others. Overlaid are results of a pQCD fit and of a fit based on a non-perturbative Regge model. The latter is able to describe the  $x$  dependence from the lowest  $Q^2$  values to about  $Q^2 = 0.65 \text{ GeV}^2$ . The fit based on the DGLAP evolution equations results in a satisfactory description of data down to  $Q^2 = 0.9 \text{ GeV}^2$ . This comes as a surprise: previous to the on-come of HERA, pQCD was expected to breakdown already for  $Q^2$  values below  $\sim$  few  $\text{GeV}^2$ .

Figure 2 shows the slope of  $F_2 / \ln Q^2$  versus  $x$  or  $Q^2$ . Coming from large  $x$ , the slopes increase when going to smaller  $x$ , remain constant for  $x$  values between approximately  $10^{-4}$  and  $10^{-3}$ , and then decrease again for yet smaller values of  $x$ . This behavior seems to indicate a transition at  $Q^2$  between 1 and 10  $\text{GeV}^2$ . The transition is not described by the GRV94 structure function and might indicate the break down of pQCD. However, a fit based on the DGLAP evolution equations to the ZEUS  $F_2$  data sets (including the present data) and fixed target data is able to reproduce the change in behavior. The transition has also been interpreted as evidence for parton recombination, but, as mentioned above, this effect is not needed to explain the features of the currently available data.

*ii) Forward Jet Production in Deep Inelastic Scattering at HERA*

The inclusive forward jet cross section in deep inelastic scattering has been measured in the region of  $x$  between  $4.5 \times 10^{-4}$  and  $4.5 \times 10^{-2}$ . This measurement is motivated by the search for effects of BFKL-like parton shower evolution. In Figure. 3 the cross section at the hadron level as a function of  $x$  is compared to cross sections predicted by various Monte Carlo Models. An excess of forward jet production at small  $x$  is observed, which is not reproduced by models based on DGLAP parton shower evolution, such as LEPTO MEPS and HERWIG.

# ZEUS 1995



**Figure 1.** Low  $Q^2$   $F_2$  data for different  $Q^2$  bins together with the ZEUS Regge fit. Also shown at larger values of  $Q^2$  is the ZEUS NLO QCD fit based on the DGLAP evolution equations.

## ZEUS 1995

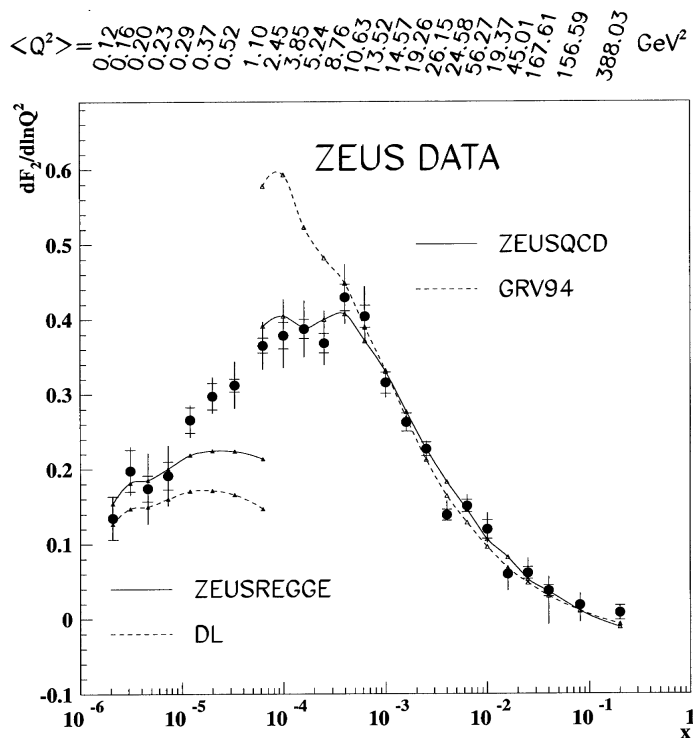


**Figure 2.**  $dF_2/d\ln Q^2$  as a function of  $x$  calculated by fitting ZEUS  $F_2$  data in bins of  $x$  to the form  $\alpha + b \ln Q^2$ . The DL and GRV94 calculations, shown as points linked by dashed lines, are from the Donnachie-Landshoff Regge fit and the GRV94 NLO QCD fit, respectively. The ZEUS QCD fits are based on the DGLAP evolution equations and include the present data. In all cases the points are obtained using the same weighted range of  $Q^2$  as for the experimental data.

## ZEUS 1995

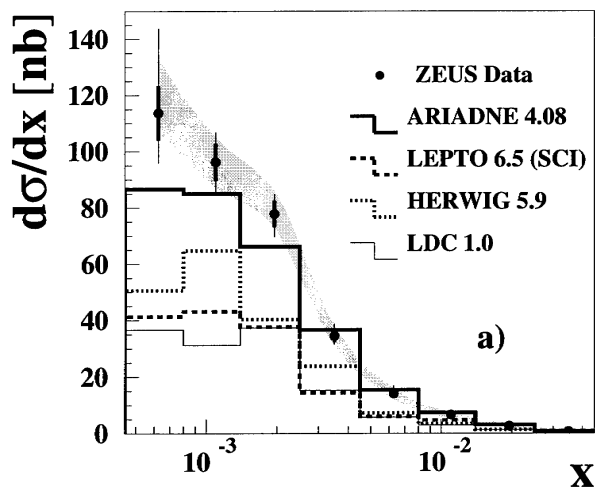


**Figure 3.** Forward jet cross section at hadron level as a function of  $x$ . The errors due to the jet energy scale are shown as the shaded band.



iv) *Measurement of the Diffractive Cross-Section in Deep Inelastic Scattering using ZEUS 1994 Data*

The DIS diffractive cross section has been measured in the mass range  $M_X < 15 \text{ GeV}$  for  $\gamma^* p$  cm energies  $60 < W < 200 \text{ GeV}$  and photon virtualities  $Q^2 = 7$  to  $140 \text{ GeV}^2$ . Here  $M_X$  denotes the mass of the diffractive system. For fixed  $Q^2$  and  $M_X$ , the diffractive cross section rises rapidly with  $W$ ,  $d\sigma_{\gamma^* p \rightarrow X_N}^{\text{diff}}(M_X, W, Q^2)/dM_X \propto W^\alpha$  with  $\alpha = 0.507 \pm 0.034_{-0.046}^{+0.155}$ , corresponding to a t-averaged pomeron trajectory of  $\bar{\alpha}_P = 1.127 \pm 0.009_{-0.012}^{+0.039}$  which is larger than  $-\bar{\alpha}_P$  observed in hadron-hadron scattering. The  $W$  dependence of the diffractive cross section is found to be the same as that of the total cross section for scattering of virtual photons on protons, see Figure 5. The data are consistent with the assumption that the diffractive structure function  $F_2^{\text{D}(3)}$  factorizes according to  $x_P F_2^{\text{D}(3)}(x_P, \beta, Q^2) = (x_0/x_P)^n F_2^{\text{D}(2)}(\beta, Q^2)$ . Here  $x_P$  denotes the fraction of the proton's momentum carried by the Pomeron,  $\beta$  denotes the fraction of the Pomeron's momentum partaking in the hard scattering process, and  $n$  describes a constant to be determined from the data. They are also consistent with QCD based models which incorporate factorization breaking. The rise of  $x_P F_2^{\text{D}(3)}$  with decreasing  $x_P$  and the weak dependence of  $F_2^{\text{D}(2)}$  on  $Q^2$  suggest a substantial contribution from partonic interactions.

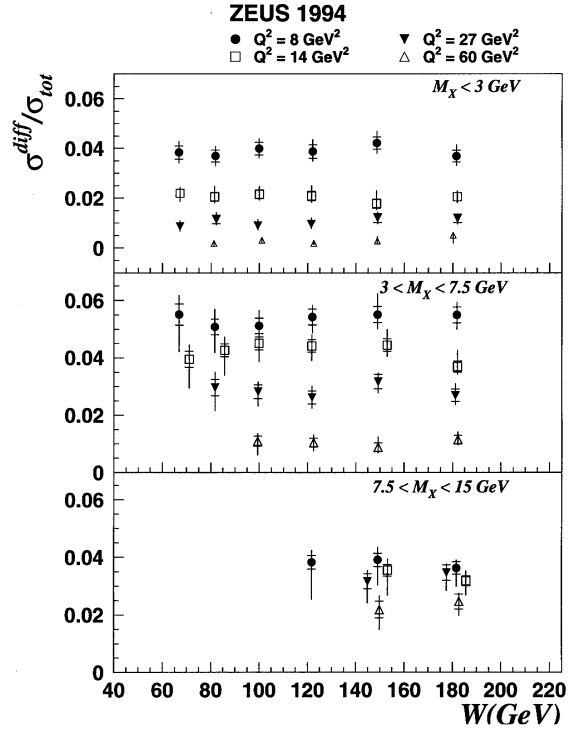


**Figure 5.** The ratio of the diffractive cross section, integrated over the  $M_X$  interval indicated, to the total cross section for virtual photon proton scattering, as a function of  $W$  for the  $Q^2$  values indicated.

v) Exclusive Electroproduction of  $\rho^0$  and  $J/\psi$  Mesons at HERA

Exclusive production of  $\rho^0$  and  $J/\psi$  mesons has been studied in the kinematic range  $0.25 < Q^2 < 50 \text{ GeV}^2$ ,  $20 < W < 167 \text{ GeV}$  for the  $\rho^0$  data and  $2 < Q^2 < 40 \text{ GeV}^2$ ,  $50 < W < 150 \text{ GeV}$  for the  $J/\psi$  data. The  $W$  dependence of the production cross section is particularly interesting since phenomenological models based on Pomeron exchange and calculations based on pQCD predict different behaviors. The  $W$  dependence of the  $\gamma^* p \rightarrow \rho^0 p$  cross section exhibits a slow rise with  $W$  at low values of  $Q^2$ , see Figure 6. Parametrising the cross section as  $\sigma \propto W^\delta$  yields the fit result  $\delta = 0.12 \pm 0.03 \pm 0.08$  for  $Q^2 = 0.47 \text{ GeV}^2$ . This value is consistent with that measured in photoproduction and with predictions based on soft Pomeron exchange. The slope becomes steeper with increasing  $Q^2$ . For  $3.5 < Q^2 < 13 \text{ GeV}^2$ , the average value of  $\delta$  is  $0.42 \pm 0.12$ . This is less steep than the value of  $\delta = 0.92 \pm 0.14 \pm 0.10$  measured in  $J/\psi$  photoproduction. The cross section for  $J/\psi$  electroproduction has a  $W$  dependence consistent with the steep dependence found in photoproduction and consistent with expectations based on pQCD.

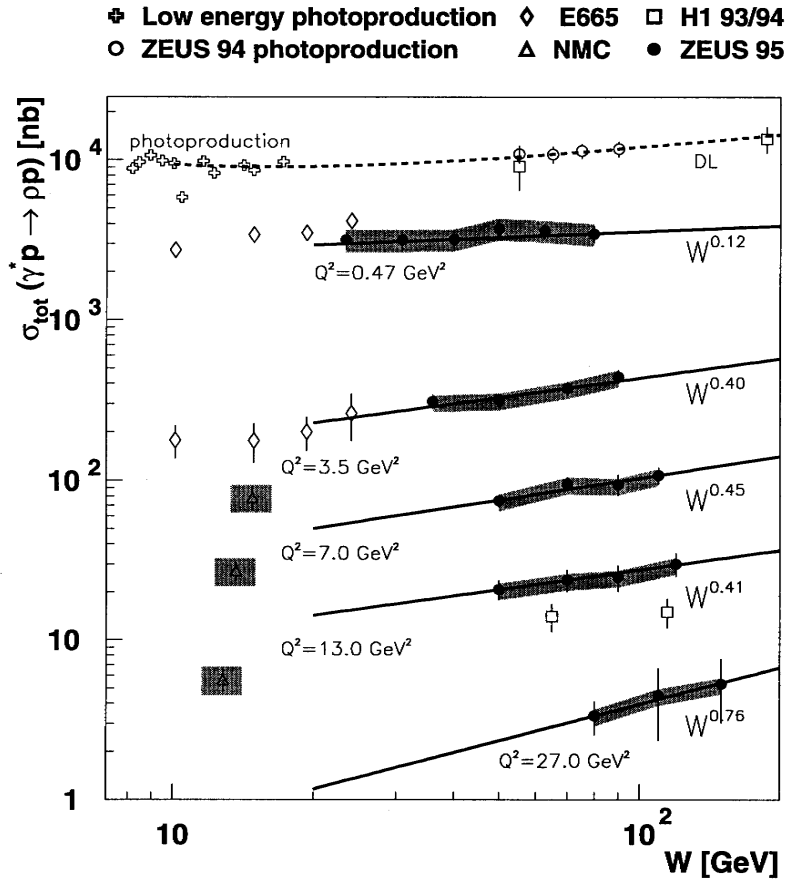


**Figure 6.** Comparison of cross sections for exclusive  $\rho^0$  production, as a function of  $W$  for various values of  $Q^2$ . The dashed line is the prediction by Donnachie and Landshoff. The solid lines represent the fitted parameterization assuming  $\sigma \propto W^\delta$ .

*Measurement of Inclusive  $D^{*\pm}$  and Associated Dijet Cross-sections in Photo-production at HERA*

Inclusive photoproduction of  $D^*$  mesons has been measured for photon-proton center-of-mass energies in the range  $130 < W < 280$  GeV and photon virtuality  $Q^2 < 1$  GeV<sup>2</sup>. Total and differential cross sections as functions of the  $D^*$  transverse momentum and pseudorapidity are presented in restricted kinematical regions. The data are compared with next-to-leading order pQCD calculations using the “massive charm” and “massless charm” schemes. The measured cross sections are generally above the NLO calculations, in particular in the forward (proton) direction. As a result of studies of dijet production associated with charm, evidence for a significant resolved as well as direct photon component contributing to the cross section was found. Figure 7 shows the differential cross section versus  $x_\gamma$ , the fraction of the photon partaking in the production of the dijet system. Leading order Monte Carlo calculations indicate that the resolved contribution arises from a significant charm component in the photon. Comparison with a massive charm NLO parton level calculation shows an excess in the data in the kinematical region where the resolved photon contribution is dominant.

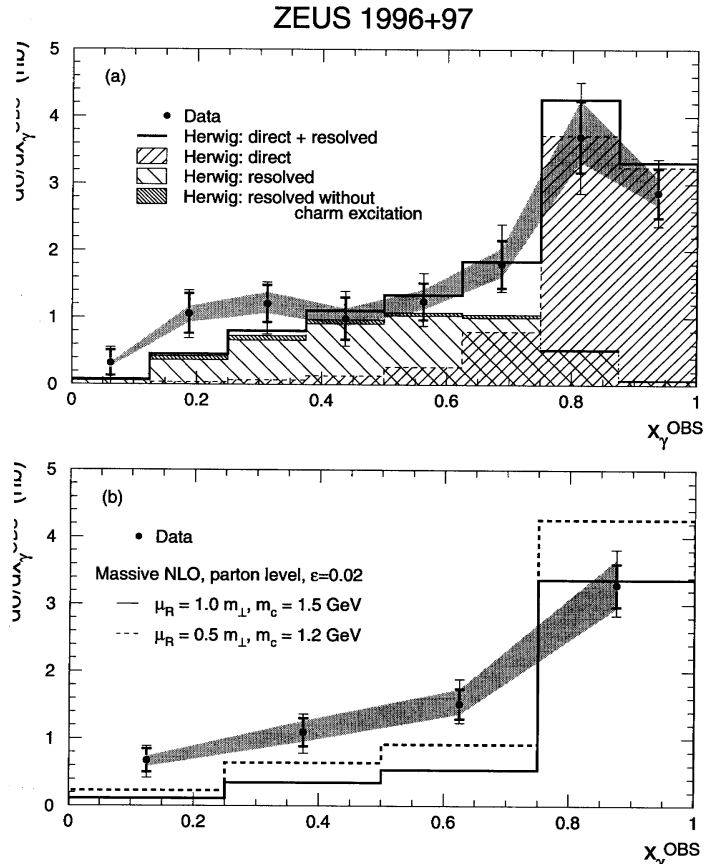


**Figure 7.** The differential cross section versus  $x_\gamma$  for dijets with an associated  $D^*$  meson. In (a) the experimental data are compared to the expectations of the HERWIG Monte Carlo simulation. In (b) the data are compared with a parton level NLO massive charm calculation.

## **b. HERA and ZEUS Operations**

In the early part of calendar year 1999 HERA continued the electron run commenced in 1998. A total luminosity of  $17.1 \text{ pb}^{-1}$  was delivered in the first four months. Thereafter the machine switched back to positron running motivated by arguments related to different marginal deviations from Standard Model expectations observed in previous positron data. No significant amount of luminosity with positrons was delivered in the remainder of the first half of the year.

The ZEUS detector performed well in this period. The recently added components, such as the forward plug calorimeter and the barrel presampler, were fully operational.

(J. Repond)

## **I.B. EXPERIMENTS IN PLANNING OR CONSTRUCTION**

### **I.B.1 MINOS -Main Injector Neutrino Oscillation Search**

The MINOS experiment is designed to search for neutrino oscillations with a sensitivity significantly greater than has been achieved to date. The phenomenon of neutrino oscillations allows the three flavors of neutrinos to mix as they propagate through space or matter. The MINOS experiment is optimized to explore the region of neutrino oscillation parameter space (values of the  $\Delta m^2$  and  $\sin^2(2\theta)$  parameters) suggested by previous investigations of atmospheric neutrinos: the Kamiokande, IMB, Super-Kamiokande and Soudan 2 experiments. The study of oscillations in this region with a neutrino beam from the Main Injector requires measurements of the beam after a very long flight path. This in turn requires an intense neutrino beam (produced by the new Fermilab Main Injector accelerator) and massive detectors. The rates and characteristics of neutrino interactions are compared in a “near” detector, close to the source of neutrinos at Fermilab, and a “far” detector, 730 km away in the underground laboratory at Soudan, Minnesota. The neutrino beam and MINOS detectors are being designed and constructed as part of the NuMI (Neutrinos at the Main Injector) Project at Fermilab.

The MINOS detectors are iron-scintillator sandwich calorimeters, with toroidal magnetic fields in their thin steel planes. The combination of alternating active detector planes and magnetized steel absorber planes has been used in a number of previous neutrino experiments. The MINOS innovation is to use scintillator with sufficiently fine transverse granularity (4-cm wide strips), so that it provides both calorimetry (energy deposition) and tracking (topology) information. The 5,400 metric ton MINOS far detector is also much more massive than previous experiments. Recent advances in extruded scintillator technology and in pixilated photomultipliers have made such a detector feasible and affordable for the first time.

Through June of 1999, results from Super-Kamiokande, Soudan 2 and MACRO experiments provide increasing evidence that neutrino oscillations are taking place in just the regions of parameter space that MINOS was designed to explore. This has provided mounting impetus to go forward with MINOS as expeditiously as possible. Earlier indications from Super-Kamiokande data had raised the possibility that  $\Delta m^2$  is below  $10^{-3} eV^2$ , but the latest data puts the best fit back up to  $3.5 \times 10^{-3} eV^2$ . Efforts at designing a lower energy beam to cope with lower values of  $\Delta m^2$  have proved useful for some physics tests at this value of  $\Delta m^2$ , so the beam spectrum when the experiment starts is a matter of continuing study.

Since the MINOS collaboration completed a Department of Energy Baseline Review of the NuMI Project during the last quarter of 1998, attention within the collaboration has turned to division of the responsibilities for the construction of the detector. Besides a host of administrative functions, Argonne physicists have been primarily involved in three aspects of preparation for MINOS: scintillator factory development, front end electronics, and the use of the Soudan 2 detector, also known as THESEUS.

Since an Argonne MINOS group member serves as WBS Level 2 manager for electronics, Argonne HEP took primary responsibility for the front end electronics. We produced a conceptual design and undertook costing and schedule evaluations for a new design using discrete components to replace the baseline concept in the TDR, due to new performance specifications. In addition, the alternative of using the IDE chip was evaluated for possible cost savings. A MINOS committee was set up to study the physics implications of the two designs. Previous work on the design of front end electronics had been done by UK members of the collaboration. The ANL group carried on this process with engineering help from Fermilab. A prototype front end electronics board was developed and tested. Important parameters were the noise and shaping time. This work is geared towards a decision on front end electronics in the 2<sup>nd</sup> half of 1999.

The second major focus of work by the Argonne MINOS group was the engineering design and prototyping of critical parts of the scintillator detector system. Argonne physicists and engineers serve as NuMI Project Level 3 WBS Managers for the scintillator strip fabrication and for the design and construction of the machines needed to construct scintillator modules. Argonne finished work on a prototype production facility for scintillator "modules" in Building 366. That facility will be used in July of 1999 to produce scintillator modules for the 4-plane prototype at Fermilab.

An Argonne MINOS group member also serves as WBS Level 2 manager for far detector installation. Far detector installation work during this period involved close interaction with the architect engineering firm, CNA Consulting Engineers, which advertised and accepted a bid for the new MINOS cavern, including its infrastructure and the detector support structure.

The Argonne installation group also continued to work on the design of installation procedures for the detector at Soudan, in close collaboration with the Soudan 2 mine crew and with CNA.

Finally, Argonne physicists have been heavily involved with preparations for MINOS excavation work at Soudan, particularly as it impacts continued operations of the Soudan 2 detector. Data from a series of test blasts in 1998 were used to provide specifications on vibration monitors for the MINOS construction bid. These specifications did not increase the cost or affect the schedule of the MINOS cavern excavation.

(M.C. Goodman)

## **I.B.2 ATLAS Detector Research & Development**

### **a. Overview of ANL ATLAS Tile Calorimeter Activities**

Despite some early setbacks, the TileCal subsystem again met many key project objectives in the first half of 1999: all 41,000 master plates for the extended barrel calorimeters were delivered to the submodule construction sites; we took delivery of all spacer plates from IFAE, Spain; we completed all essential submodule construction tooling and commenced production of submodules at the beginning of February and a total of 34 submodules were stacked and glued in this period; the procurement for the strongback girder was placed and we expect delivery of the first two in August; the plans for shipping modules to MSU and to CERN have been fully developed and detailed design of the transporter and shipping beams is underway; work on preparing the instrumentation area is in progress and the scheme by which modules are moved into the area finalized; finally, in collaboration with a student, R. Stanek has completed some essential R&D tests to confirm the feasibility of using an LED system rather than a radio-active source to perform quality control checks during module instrumentation.

(J. Proudfoot)

## **I.C. DETECTOR DEVELOPMENT**

### **I.C.1 The CDF Upgrade Project**

Shower max calorimeter readout continues a major project for us; Karen Byrum has become project manager along with Gary Drake being Chief Engineer. Gary did the testing which showed that at least one of the production chips for the shower max current splitter and ADC ASIC “SMQIE” actually works. A new version of his boards “SQUID”, which mount these production chips, is being prepared. John Dawson has brought the VME readout boards “SMXR”, which interface to the “SMC” cards that house the SQUID cards, ready for production.

A difficulty, which resulted from timing problems due to implementing revisions, has been fixed in the FPGA programming. Steve Kuhlmann, Jimmy Proudfoot, and Jim Schlereth, working with John and Gary, put together a system test and developed software for readout and calibration of the whole system, as well as for production testing of SMXRs. Some of this effort has been replicated as part of the “Wedge Test” at B0.

Karen continues working with Gary to develop the amplifiers needed for the wire chamber shower max readout; a scheme which is acceptable for wires and within a factor of two in gain or noise for strips has been demonstrated and a different idea is being developed. The test checks the strip-to-wire pulse height ratio using  $^{55}\text{Fe}$  on a shower max strip chamber as seen in Figure 1.

Karen and John have been working with the Michigan group to prototype the shower max Level 2 trigger bit input; this has been demonstrated using Level 2 emulation. John is also working with the Yale group on the Level 1 interface to Level 2. Steve, John, and Bob Blair have prototypes of isolation trigger electronics, which could well end up usable. Larry Nodulman, along with Jim Van Howe a summer student, have been rerouting and shielding wire chamber signal cables, and redoing grounding on the detector. Several crack chambers that had high voltage problems were replaced. One further crack chamber installation awaits suitable placement of the calorimeter arches.

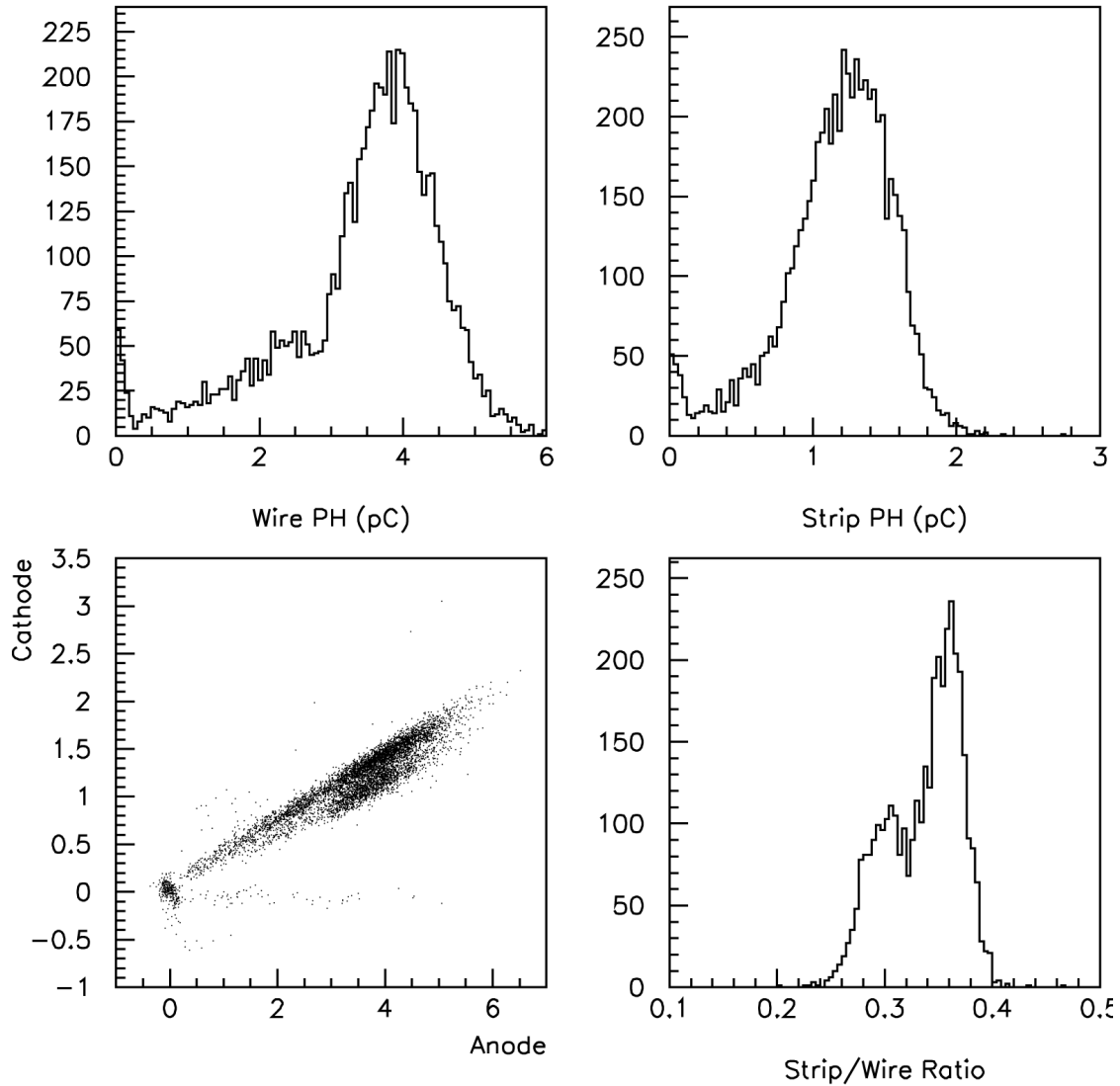


**Figure 1.** Wire and strip pulse height in picocoulombs, and the correlation and ratio which shows  $^{55}\text{Fe}$  x-ray conversions above and below the wire.

Bob Wagner and Randy Thurman-Keup have been developing offline software for calorimeter reconstruction with emphasis on the electron code. Steve and Barry Wicklund are becoming involved in code for the wire chamber data reconstruction.

Bob Wagner demonstrated that the diode protection system in the central EM phototube bases causes a noticeable nonlinearity in the high energy range, which may become important with the larger Run II data samples. A plan for fixing the bases and checking the tubes has begun with Bob supervising summer help at Fermilab.

Randy has continued work with the central drift chamber group “COT” at Fermilab in using tooling we developed for inserting the wire planes and field sheets into the can

of the chamber. The stringing was complete when it was discovered that the wire plane end card alignment features called “nibs”, which provide alignment with a groove in the end plate slots, were not robust. Many of the ends need to be reseated, and some nibs need to be replaced. These repairs have begun. We are working on a design for a folded up insertion engine, suitable for use after the COT has been mounted in the solenoid.

Randy has also taken charge of high voltage control for wire chambers other than COT, which includes muon chambers as well as preshower, shower max, and crack chambers in our calorimeter.

Good progress continues on the muon upgrade, under the oversight of Tom LeCompte. New front end electronics and chambers are completed and installed. The new intermediate system chambers are complete and being installed. Some of the old muon scintillators, which will now be needed for bunch identification, have deteriorating plastic. These have been repaired by adding wave shifting fibers.

(L. Nodulman)

## **I.C.2 ZEUS Detector Upgrade**

### **a. Straw Tube Tracker Readout Electronics**

ZEUS plans to install a new forward tracking detector during the 2000/2001 machine shutdown. The new tracker is based on the straw tube technology and will consist of 48 sectors containing a total of 12,000 tubes. It is expected to greatly improve the detector's ability to measure high  $Q^2$  neutral current events, to determine charged current event vertices, to tag heavy flavor decays in the forward direction, and to track charged particles in general. The detector is being built by a group of nine institutions that are all part of the ZEUS collaboration.

The Argonne group took over the responsibility of designing and building the front-end electronics consisting of shapers, discriminators, a multiplexing and a cable driver circuit. The multiplexing is necessary to match the 12,000 channels of the new detector to the 2,000-channel readout system of the current forward detector.

As a first step Argonne built a prototype board containing the two-threshold ASDBLR chip developed by University of Pennsylvania to shape and discriminate the signals, and a circuit to drive the standard 42 m signal cable employed by the experiment.

Based on experience gained with the first prototype, a second prototype is being developed using the ASDQ chip, which contains a one-threshold discriminator. The second

prototype will contain all elements of the readout system, including the multiplexing circuitry, and should be very similar to the final production electronics.

(J. Repond)

### **I.C.3 ATLAS Calorimeter Design and Construction**

#### **a. Calorimeter Construction**

##### *i) US Master Plate Stamping*

All master plates were delivered to submodule construction sites in Europe and the United States. Following the corrective action with regard to banding and blocking of the pallets, no further problems were encountered during shipping. The full data set of quality control data obtained by computer measurements of a subset of the stamped plates was analyzed to characterize the as-built plates against the design specification. An Argonne technical report (ANL-HEP-TR-99-04) was written. The plates are exceptionally reproducible. The width of the outer radius key as a function of stamped plate (production period) is shown in Fig. 1. The distribution has a mean of 181.031mm with an rms of 0.018mm to be compared with the allowed design specification of 181.0-181.1mm. The data for the earlier production of plates for the barrel modules are essentially identical with a corresponding mean of 181.038mm and rms of 0.018mm.

##### *ii) Submodule Small Components*

Several of the components required for submodule construction are the responsibility of our European collaborators. These include:

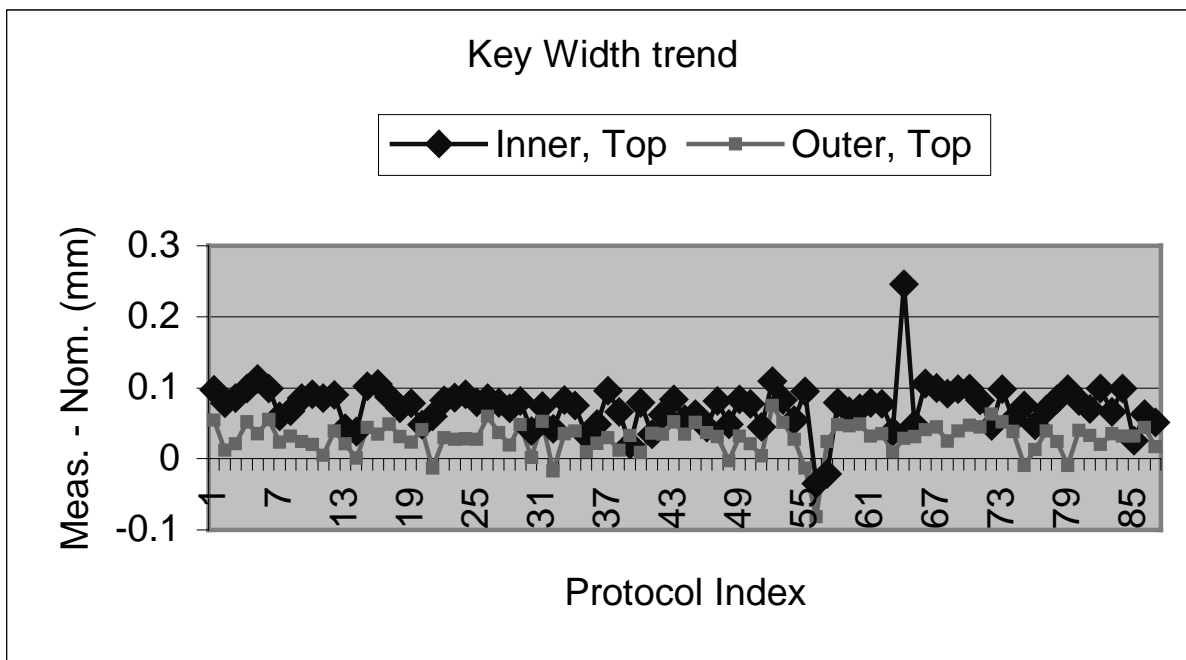


**Figure 1.** Inner and outer key width for each of the 87 plates measured on a computer measuring machine as part of stamping production quality control.

- Spacer plates from Spain: full delivery of these has been made.
- Structural adhesive from CERN: the initial delivery has been made.
- Small keys via CERN: the initial delivery has been made.
- Spring pins from CERN: the full delivery has been made.
- Protective paint via CERN: an initial delivery was made, however, the paint was defective and replacement paint is being shipped in July.

In the U.S., we are responsible for fabrication of the weld straps used in the assembly of modules constructed here. This is a joint UTA/ANL task in which ANL has responsibility for the bar stock procurement through CERN and UTA the responsibility for cutting and machining the bars.

The first bars were made on schedule. However, during submodule construction, it was noted that the hole positions, bar lengths, and widths were not consistently meeting the design specification. We engaged in extensive discussions with technical staff at UTA to understand the cause of these deficiencies, which were determined to be resulting from problems in both the machine and the fixturing, and tooling being used. Both equipment problems were corrected and we initiated a more exacting quality control at the UC machine shop that has eliminated all problems except those of human error.

### iii) *Submodule Production*

Submodule construction commenced somewhat behind schedule in early February. It was immediately apparent from the first production submodule constructed at Argonne, as well as those constructed at other locations, that the design stack height could not be met. Following some detailed measurements and a thorough review of the impact of design changes on other elements, the design height of the stack was reduced to 291.7mm and submodule production restarted at the beginning of March. The change is attributed to a small decrease in the raw plate average thickness plus a contribution from the plates being flatter than those used for the prototype program. Thirty-four submodules have been stacked and glued and we have achieved our planned production rate of 3 submodules per working week using a crew of 2 technicians and one lead technician.

Many other more minor startup problems were encountered:

- Attention to the orientation of master and spacer plates (solved by more explicit definition of plate orientation during stacking *vis-a-vis* the stamping direction).
- Maintenance of the glue line (solved by use of paper shims).
- Distortion at the inner radius (partially solved by use of thin steel shims).
- Location of the weld bars on the submodule.
- The smoothness of operation of the glue machine (including motors, backlash, and humidity effects on the glue viscosity and blockage of the dispenser). Since this also affected the length of time required to stack a submodule, some reworking of the glue motors and controls is planned to be carried out in the fall.
- The effectiveness with which the Timesaver machine cleaned plate edges (largely solved by addition of customized spray heads).
- The operation of the Timesaver machine to process small plates (largely solved by adding some custom rollers at the exit stage of the machine).

In addition, there were two major problems. The first was with the failure of the initial weld bars fabricated by UTA to meet specification. This has been discussed above and the issue is now largely resolved. The second major problem was with the application of a protective paint. This paint is supplied from the Czech Republic and the first batch was determined to have been damaged (by freezing) during shipment and gave a very poor coverage. The painting procedures themselves were also suspect and subjected to intensive review by our European collaborators in this period. An attempt by us to use paint from a US supplier was not particularly successful. The procedures themselves are now fairly well established and we expect to take delivery of a new batch of paint in August. At the present time this is the only major outstanding production problem.

iv) *Submodule Quality Control*

The QC procedure document was completed and accepted by the Tile Collaboration as a basis for a subsystem-wide approach for verification of submodule construction. The procedure includes a detailed set of height measurements as well as a systematic check on the height of the scintillator slots, the welding, and on painting. The data are regularly updated on a web-based database and J. Proudfoot is presently designated as the overall monitor of production activities. One of the more important dimensions being monitored is the submodule height as measured at 20 different locations. A typical distribution of heights averaged over 34 submodules is shown in Fig. 2. Points 7 and 14 are at the inner radius where we associate the increased shrinkage with distortion during welding. Several attempts were made to reduce this distortion since it is expected to have an adverse effect on the instrumentation procedures, but at the present time no significant improvements have been achieved. This distortion, in addition to better control of the scintillator slots at the inner radius, are issues which will continue to be studied in the second half of 1999.

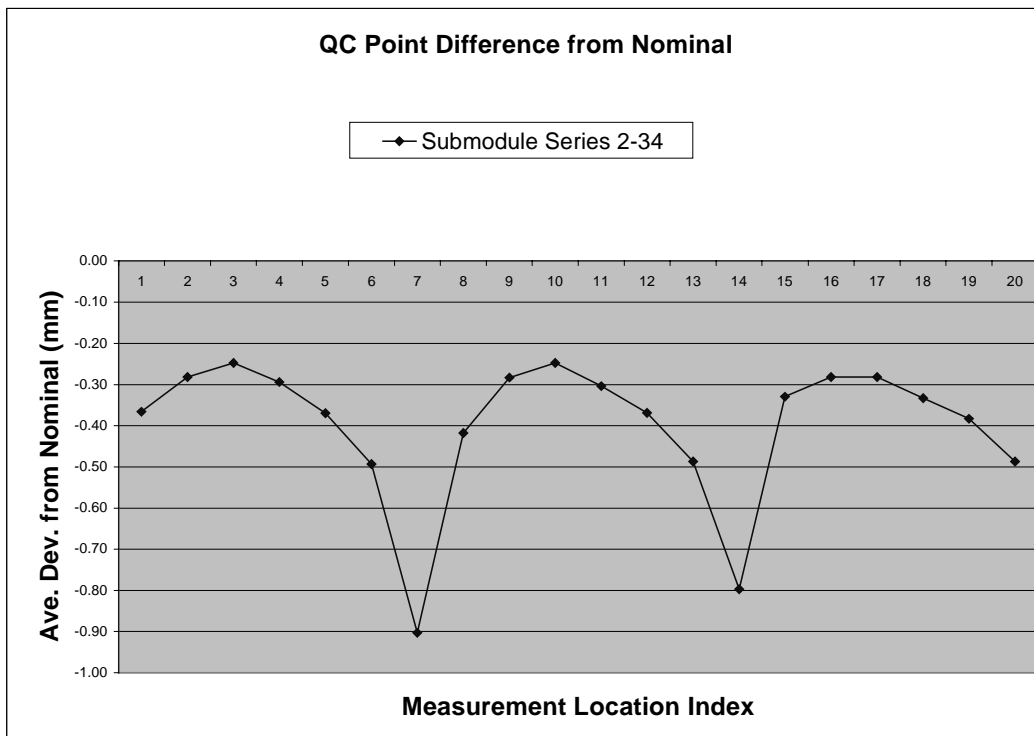


**Figure 2.** Submodule height quality control data.

In addition to the TileCal weld procedures, the technical staff at Argonne have fabricated several simple tools to facilitate clean out of glue from the scintillator slots. Many procedures were written and include procedures for use and maintenance of the Timesaver machine, glue machine, and stacking fixture. The lead technician also wrote and uses several checklists to ensure the correct sequence and execution of construction activities. Finally,

though not technically a QC area, the group also gave written and oral presentations to the ANL-HEP Division Safety Review Committee as part of the Division procedure for commencing construction activities.

v) *Module Construction*

We have commenced building layout and assembly of the tooling to construct modules. The assembly base is aligned and installed, our optical transit calibrated, and a precision beam is being modified to allow for easier use in module envelope control. Most of the module components have been ordered and, in particular, the order for the strongback girders has been placed with the Spanish vendor who is providing the girders for the extended barrel modules that are being constructed in Europe. In an attempt to bring module production back onto schedule, we plan to air-freight the first two production girders to Argonne at the beginning of August.

vi) *Module Shipping*

Work continued in this period to develop the plan and hardware for shipping modules to and from MSU and to CERN.

The scheme to ship modules to MSU was finalized and is based on a transporter that will be designed and built by MSU, allowing them to lift and move modules from the back of a flatbed truck onto their loading dock and from there into their assembly area. The main discussion between ANL engineers and the MSU staff has focussed on issues associated with the stresses in the structural elements. As a result, there have been several changes in the detailed design of the lifting beam that forms a critical structural element in the transporter and which must simultaneously allow their use as support beams during road transportation. It is expected that the transporter will be constructed by late September.

We have continued to hold discussions with the regular Argonne brokerage firm for overseas shipments (American Overseas Transport) on the best and most cost-effective approach for the shipment of modules to CERN. We have decided to use this company on a shipment-by-shipment basis to handle all aspects (packaging, over-ocean shipping, and transportation to the CERN site), as we neither have the expertise or the resources in-house. We will host a meeting with all parties concerned later in the year to review the requirements.

(J. Proudfoot)

## **b. Calorimeter Instrumentation and Testing**

Work continued on the preparation of the Argonne instrumentation area, and the purchase of supplies and one-time infrastructure items. Also, comparisons of two different quality control tests were performed.

The instrumentation of a single sub-module in a light-tight box, which was begun last year, continued. Fibers were prepared and put into profiles at Argonne. Profiles are the plastic sleeves that serve to both hold the fibers in place, and make a reflector for better light collection from the tiles. Half the fibers we used were aluminized at Fermilab, and half were made reflective on one end with white-out. The fibers were routed to 6 phototubes so that each side of the three calorimeter cells could be read out separately. This module was read out with signals from a radioactive source that could be positioned in the source tubes by remote control. This was done initially by Bob Stanek and is written up elsewhere in this report.

Preparation for instrumentation involves ordering quantities of such things as optical epoxy, special cable ties in large quantities, brass rods for fiber support on the modules, etc. We began ordering infrastructure items such as a PAL video monitor, 220 power converters, and power supplies for the polishing machine that cuts and polishes the fibers inside the girder. The ordering of infrastructure items is going slowly because, in many cases, the exact specifications are not available from CERN or other institutions. Also, in many cases the specifications are metric or involve European suppliers, and ANL and MSU are working together to find US suppliers of equivalent items.

The light tight tent to be used for the QC measurements was finished. We have not yet tried to mount it in the instrumentation room for several reasons. There are no lights in the room because the electricians are not available. The plan for mounting has changed since we changed the instrumentation plan from moving modules by trolley or fork lift to moving them by crane through a hole in the roof of the room.

There is ongoing work at Argonne to prepare the readout of the test electronics drawers, which will be used for QC during production. This involves R. Stanek and two students, and is written up in a separate section of this report.

(D. Underwood)

## **c. Test Beam Program**

A June/July testbeam run was started with the main intention of verifying that the pre-production on-board digitizers are of sufficiently good design to go into production. The

barrel Module 0 was installed in H8 after having repairs made to several tile/fiber couplings. Latest Version 3-in-1 cards were installed, as well as several latest generation Hamamatsu R5800 PMTs. Unfortunately, at the start of the run, the digitizers were not available, and the backup FERMI readout was used.

Another goal of this testbeam run was to understand the performance of the calorimeter at low energies -  $\sim 5\text{GeV}/c$  and above. Since the beamline was designed for hundreds of GeV, the uncertainty in the low energy can be 20%. Along with CERN beamline physicists, HEP staff helped design and implement a beamline spectrometer which used beam MWPCs and a new trim magnet with a well-known  $\int B \cdot dl$ . A successful test of the spectrometer was made in June, measuring the momentum of 10 GeV electrons to  $\sim 1\%$  of the nominal momentum. This technique will be used in July for 5 GeV beam.

HEP staff took an active part in the analysis of the June/July 1998 data. Until recently, analysis activity concerned the detail mapping of the performance of the modules. We have now moved towards investigating the performance using ATLAS requirements. One such requirement is the limited number of samples to be used to reconstruct both charge and time. In order to get a baseline for the new digitizers, a study of the time resolution expected using the FERMI system was done. In Figure 3 we see that we can expect time reconstruction of  $\sim 1.5$  nsec using a very simple algorithm with the time samples and the LeCroy TDC for normalization.

#### **d. Extended Barrel QC Program**

For QC of the production modules in 366, a  $^{137}\text{Cs}$  source will initially be used to verify uniform coupling for all tiles and fibers. This procedure was followed in 1997 with Extended Barrel Module 0. The same source drive will be used. However the new HV electronics and the current integrator ADC requires the use of CAN bus protocol, while the 3-in-1 cards used a VME-based control system. A decision to use a PC-based acquisition system rather than VME resulted in cost savings as well as compatibility with collaborators in Spain.

To overcome the VME link with the 3-in-1 system, a CAN bus 3-in-1 controller was designed, built and tested by HEP staff. This controller is based on a philosophy of a general-purpose design, with HEP staff writing the 3-in-1 specific firmware for the Phillips 80C592 microcontroller, and the implementation of 3-in-1 specific timing and output signals in an Altera 10K FPLD. Four of these devices were tested and three were sent to Barcelona, Clermont-Ferrand and MSU.

An attempt will be made to phase out the  $^{137}\text{Cs}$  source and implement a blue LED to illuminate the fibers. If an LED source can be used for the quality control of the module production instead of a radioactive source, it will simplify safety procedures both at Argonne and

at the university where many undergraduates are doing instrumentation work in the laboratory. HEP staff is designing an LED assembly to be fitted to the source scanner, replacing the radioactive source but maintaining all the original functionality.

The optical test module was finally instrumented with spare scintillator and fibers from Lisbon. In order to verify the validity of using an LED rather than a source, studies were made on this test module comparing data from an LED scan and a  $^{137}\text{Cs}$  source scan. An undergraduate student at Argonne, S. Zeltich, with some assistance from a student and technician from MSU, performed these measurements. In actuality, the fiber coupling to the tiles was purposely made badly in many spots in order to test the limits of the LED scheme. In Fig. 4, we see the results of the comparison between the LED and the Cs data. We can expect that the LED will reflect the individual tile/fiber response to  $\sim 11\%$  of that predicted by unfolding the response from the Cs data. This seems quite adequate for QC at the level of 10%. Further tests will be performed on the real ATLAS modules before we at Argonne switch to using the LED exclusively.

(R. Stanek)

99/04/01

### Pions

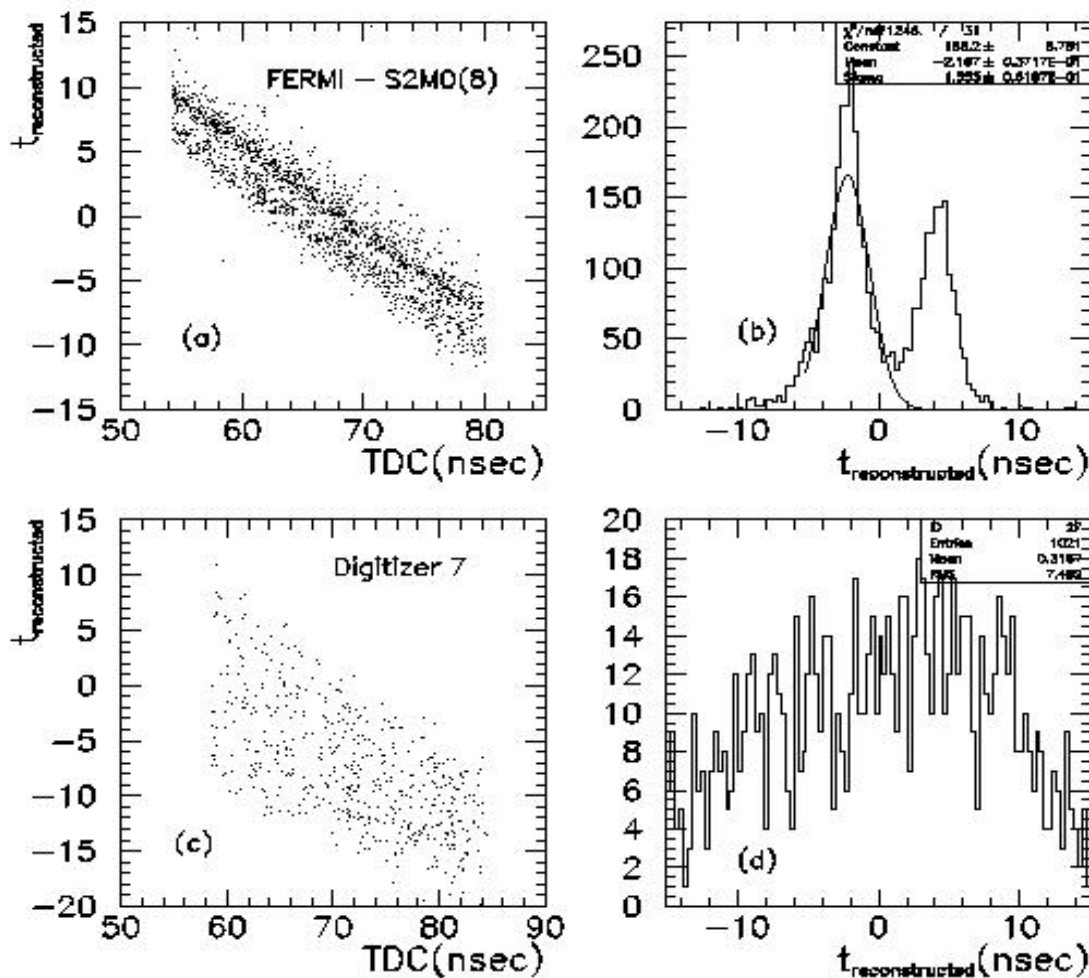


**Figure 3.** Reconstructed times using an algorithm employing three (3) samples for pion showers. (a) Reconstructed time vs. TDC. The two bands correspond to high and low gain channels having different timing. (b) The reconstructed time resolution in nsec. The reconstructed resolution is ~1.5 nsec. (c) and (d) Same as for a) and b), but for a preliminary version of the digitizers. It was discovered that the TDC did not correctly operate in the digitizer mode.

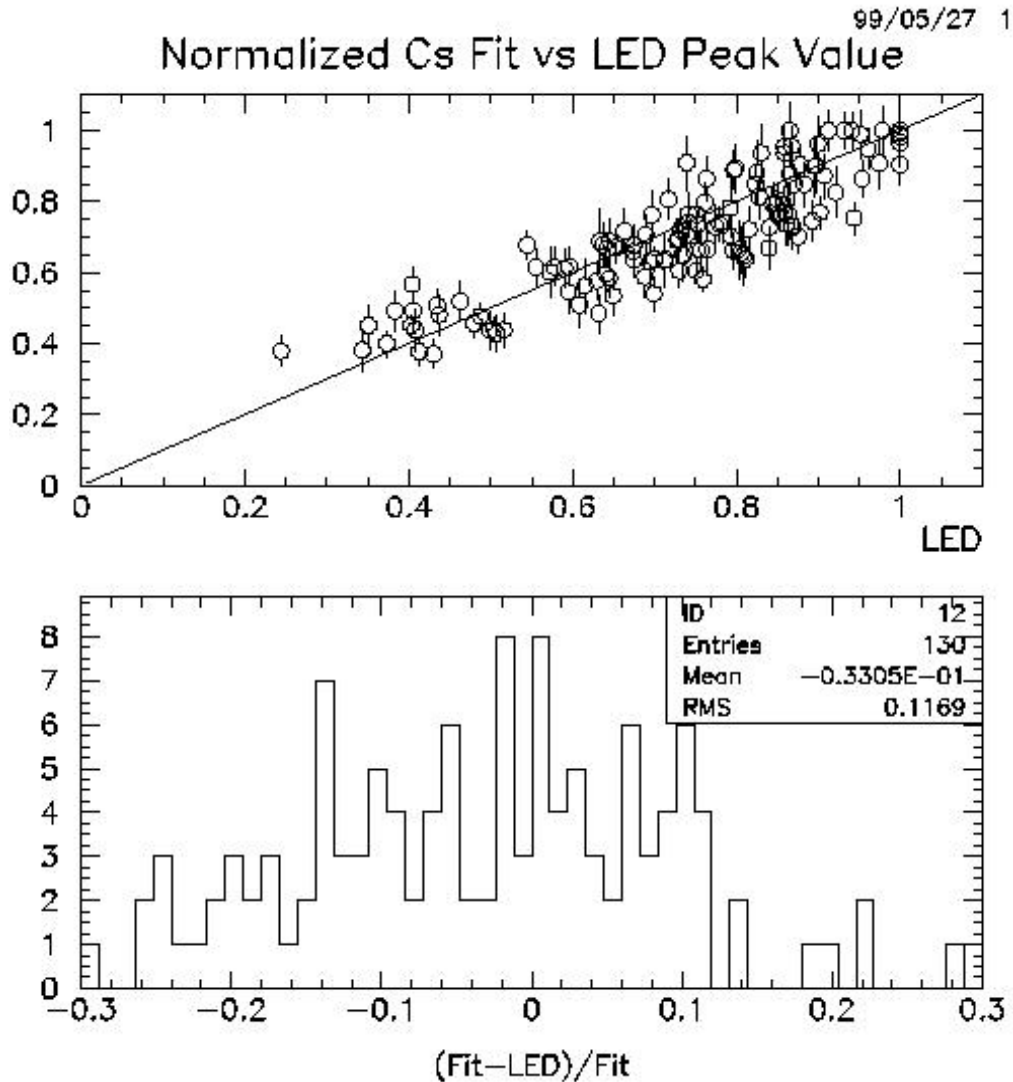


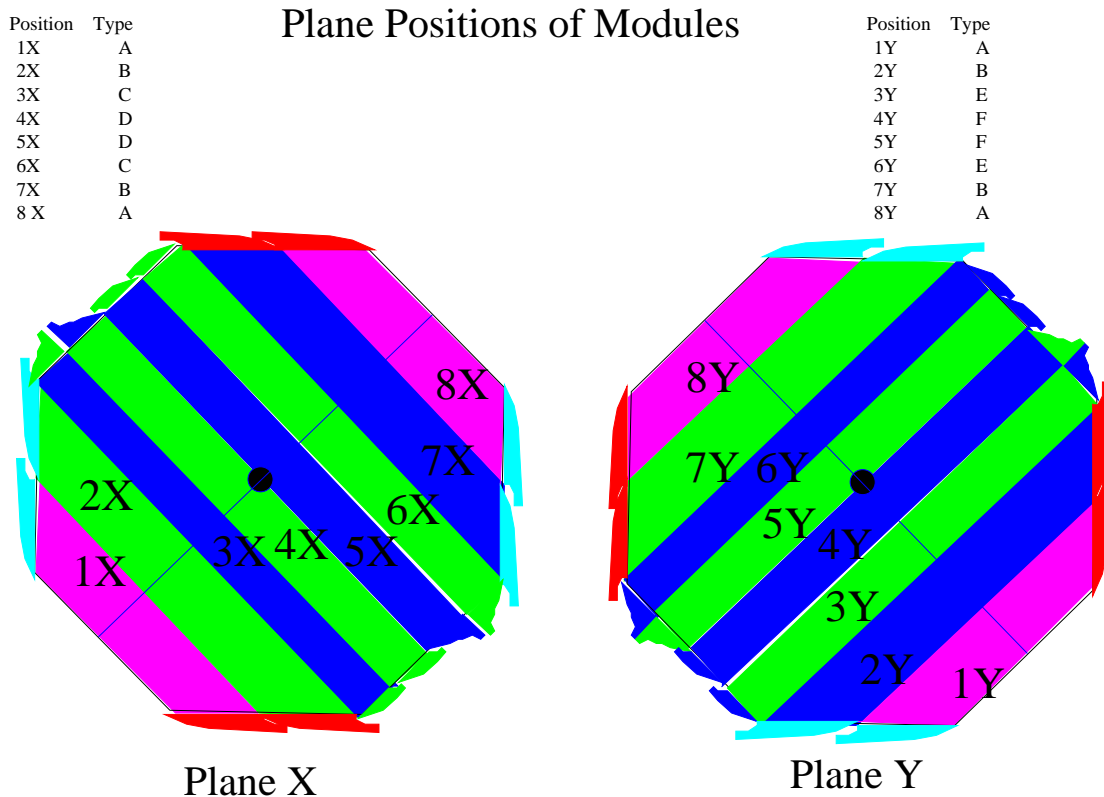
**Figure 4.** Fitted Peak parameters versus LED Peak for the optical module. The line  $y = x$  is superimposed. The bottom figure shows the correlation between the methods is 11%.

#### I.C.4 MINOS Detector Development

During the first half of 1999, the Argonne MINOS group devoted a substantial effort to meet its responsibility for the development of procedures for the production of extruded

scintillator strips, most of the assembly machines, quality control equipment and procedures which will be used at the scintillator module assembly facilities. ANL set up its prototype factory for planned use in July of 1999, in order to both make scintillator modules for the 4-plane prototype, and to benchmark module production requirements and schedules. Important operational experience was obtained on a number of devices which were developed at ANL: the semi-automatic fiber gluer for placing the WLS fibers into the grooves of each 4 cm scintillator strip, the fly cutter to make very flat surfaces on the fiber optical connections to ensure high light transmission, and the module mapper which was used to move a radioactive source at varying positions above a module and measure its response.

A major part of the effort consisted in identifying and documenting the specific module parameters relevant for a module factory. Because there are 2 different plane orientations and 8 modules per plane there could be 16 different types of modules. Thanks to rotational symmetries there are only six different types of modules and each plane only has 4 different types. This makes the construction and the mounting much easier. Each plane will contain 2 short 45-degree modules, 2 long 45-degree modules, 2 perpendicular modules and 2 bypass modules. The 45-degree modules are the same for both plane orientations. The bypass and the perpendicular modules have a handedness that depends on the orientation of the modules in the plane. Therefore there are 2 types of each of these.



These planes are laid out as if the observer is looking down on the modules mounted on the steel standing at what will become the bottom of the plane when it is hung on the supports. In this view Plane X is a v-oriented plane and Plane Y is a u-oriented plane. With the different fiber manifolds drawn, one can see the different symmetries that reduce the number of different module types from 16 to 6. Each of the different types of modules have been given a letter name. The short 45 is type A, the long 45 is type B. A plane with the v orientation will have 2 perpendicular modules of type C and two bypass modules of type D. The u orientation will have two perpendicular modules of type E and two bypass modules of type F. The lengths of every module strip in every module type was included, and the lengths of the fibers specified as part of the module production process. A large number of further conventions were developed, such as strip numbering, fiber positioning, etc. With feedback from a variety of sources, these were documented and incorporated into the tracking and quality control processes. In addition, a system of mounting “H-clips” was developed, and a system of fiducial marks for surveying was incorporated into the production process.

(M.C. Goodman)

#### **I.C.5. Electronics Support Group**

CDF: We continued with our work in the development of front-end electronics for the Shower Max Detector of the CDF Upgrade at Fermilab. For this project, we have overall responsibility for the electronics engineering of the system. The major responsibility in this project involves the coordination of the design engineering and system integration for the entire system. This includes the development of a custom integrated circuit for the front-end electronics, all of the front-end boards and crates, and the read-out board that interfaces to the upper levels of the data acquisition system. This development is a collaborative effort between Argonne and Fermilab.

Besides oversight, we are directly responsible for the specification and testing of the custom integrated circuit for the front-end electronics, called the SMQIE. Last year, we completed the testing on the final prototype chip, and gave the approval for the production of ~20,000 chips. The packaged parts are expected in July.

Argonne is also responsible for the design, testing, and production of the daughter boards that contain the SMQIEs, called SQUIDs. Each SQUID contains two SMQIEs, and also other support circuitry for calibration. Two prototypes were designed previously, for testing earlier prototype chips. The design of a new board was recently completed, which will contain two packaged SMQIE chips. The board will be tested in July when the packaged parts arrive.

Another project that Argonne has direct design responsibility for is the design and production of a VME-based readout board, called the SMXR. This is a sophisticated data processor. It receives digitized data in floating-point form from the front end electronics at the

rate of 300 Mbytes/Sec, adds together up to four words as sampled in time to reconstruct long signals from the detector spread out in time, and also forms trigger bits from the reconstructed signal. The data is stored in a buffer pending read-out by the data acquisition system. The first prototype was developed in the early part of 1998, and the design of a second prototype was recently completed. After a period of testing, we plan to begin production in the fall.

Work is in progress to put together a small system test at Fermilab. This testing will be the final shakedown of the prototype electronics before production. Much of this effort requires the generation of software, which is being written by Argonne physicists. Argonne is taking the lead role in defining and executing the qualification testing of the prototypes as a prerequisite before production.

ATLAS: We have major responsibilities in the development of electronics for the Level 2 Trigger of the ATLAS Detector at CERN. Working with colleagues from Michigan State University, we are responsible for the development of two parts of this system: the Level 2 Trigger Supervisor, and the Region of Interest (ROI) Builder.

The ROI Builder is the interface between the first level trigger and the second level trigger. When an event occurs in the detector, signals are sent from the front-end electronics to the Level 1 Trigger. The Level 1 Trigger collects event fragments from all over the detector, and stores them in a buffer. The Level 1 Trigger boards then send lists of addresses to the ROI Builder, identifying where the event data from the "Region of Interest," can be found. The ROI Builder collects the addresses for the event, and "builds" the event. It then sends the result to the Trigger Supervisor for distribution to Level 2 processors. The board is highly complex, using fast, high-density Field programmable Gate Arrays (FPGAs) to implement the functionality.

The first ROI Builder prototype was built in the fall of 1998. The board was tested at Argonne, and achieved good performance. We then built several boards to form a small system. The boards were tested at Argonne using a small computer farm that we had built previously. A large part of the testing involved writing software to control and read out the system, written by a physicist in our group. In the spring, after the successful completion of testing at Argonne, the system was sent to Saclay. It was merged with their system to create a larger network. Tests are presently underway. By the summer, the system will move to CERN for further testing. It is anticipated that the result of this phase of development will lead to a full specification of the architecture of the Level 2 Trigger System, including the Supervisor and the ROI Builder. We expect that ANL and MSU will have joint responsibility in building these pieces of hardware for the final system.

MINOS: In this last period, we continued our involvement with MINOS, the Neutrino Oscillation Experiment at Fermilab and the Soudan mine. Our group has Level 3

Management responsibility for the front-end electronics of the experiment, as well as responsibility for a large portion of the front-end design.

At the end of 1998, the collaboration was considering a choice between two types of photodetectors for the experiment: Hamamatsu 16 channel multi-anode phototubes (PMTs), or Hybrid Photodiodes (HPDs). The outcome of this decision would greatly affect the design of the electronics, since the gain of HPDs is ~1000 times less than PMTs, and the HPDs would need a custom integrated circuit in order to read it out whereas PMTs would not. In the spring of 1999, after much debate, the collaboration decided to use PMTs. Following this decision, we began planning the electronics.

Our proposal for the electronics is based on building discrete amplifiers in hybrid form. Every channel would have a low-cost ADC, and also circuitry for measuring radioactive sources. We created a conceptual design, and compiled cost and schedule plans. Working with colleagues at Fermilab, we built a prototype channel and made measurements. We presented the results at the collaboration meeting in June. We are now planning for a design review in the fall of 1999. A high priority in this project is meeting an aggressive schedule for building a small system by the spring of 2000, with production planned for the fall of 2000.

ZEUS: The ZEUS experiment at DESY is planning to replace the tracking detector in the forward region during the shut down in 2000. The new detector will use straw tubes, rather than the older-style wire chamber technology. The detector produces a pulse in response to a charged particle passing through the detector. The electronics must sense the pulse, and send a digital signal to the “back end” electronics in response, where a timestamp for the signal is recorded. This is then used to reconstruct the trajectory of the particle through the tracking detector.

In the fall of 1998, we investigated a custom integrated circuit developed at PENN, called the ASDBLR. The chip was designed for use with the tracking detector in the ATLAS experiment, and performs the front end analog signal processing. In February, we built a prototype board based around this chip, and delivered it to DESY for tests with the prototype detector in a test beam. The tests were very successful, and both the chips and the test board worked well. However, during this time, problems with procuring the ASDBLR emerged. The foundry planned to discontinue the fabrication process, and the resulting increase in cost to convert to the new fabrication process became prohibitive. It was decided to investigate other possibilities. PENN has developed another custom integrated circuit for use on the tracking chamber of the CDF experiment, called the ASDQ. We are now in the process of obtaining sample chips, and will investigate using them on the ZEUS straw tube detector.

(G. Drake)

## II. THEORETICAL PHYSICS PROGRAM

### II.A. THEORY

#### II.A.1 Single-Top-Squark Production Via R-Parity-Violating Supersymmetric Couplings in Hadron Collisions

Edmond L. Berger, Brian Harris, and Zack Sullivan developed a new method to search for a top squark, the supersymmetric partner of the top quark, and to probe  $R$ -parity-violation in supersymmetric extensions of the Standard Model. In Argonne report ANL-HEP-PR-99-05, published in Physical Review Letters **83**, 4472-4475 (1999), they examine the  $s$ -channel production of a *single* top squark through an  $R$ -parity violating mechanism. Their focus is on the relatively light top squark  $\tilde{t}_1$  and its subsequent  $R$ -parity-conserving decays. The  $R$ -parity violation penalty is paid only once, in the initial production, and is offset by the greater phase space relative to pair production.

In supersymmetric extensions of the standard model, particles may be assigned a new quantum number called  $R$ -parity ( $R_p$ ). The particles of the standard model are  $R_p$  even, and their corresponding superpartners are  $R_p$  odd. The bounds on possible  $R_p$ -violating couplings are relatively restrictive for the first two generations of quarks and leptons, but much less so for states of the third generation. If  $R_p$  is conserved, as is often assumed, superpartners must be produced in pairs, each of which decays to a final state that includes at least one stable lightest supersymmetric particle (LSP). The production rates for pairs of strongly interacting supersymmetric particles, the squarks and gluinos, benefit from the large color couplings of these superpartners to the incident light quarks and gluons in hadronic scattering subprocesses. However, in many models, the squarks and gluinos are relatively heavy, and therefore their pair production incurs a large phase space suppression.

Single-top-squark production via  $qq' \rightarrow \tilde{t}_1$  probes  $R$ -parity-violating extensions of the minimal supersymmetric standard model through the  $R$ -parity-violating coupling strengths  $\lambda''_{3ij}$ . Beginning with the superpotential for  $R$ -parity-violating couplings, Berger, Harris, and Sullivan write the partonic cross section for the process  $qq' \rightarrow \tilde{t}_1$  and compare with that for pair production. Then discussing observability, they focus on one clean  $R_p$ -conserving decay,  $\tilde{t}_1 \rightarrow b\tilde{\chi}_1^+$ , with  $\tilde{\chi}_1^+ \rightarrow l^+ + \nu + \tilde{\chi}_1^0$ . Here,  $l$  is an electron or muon, and the  $\tilde{\chi}_1^+$  and  $\tilde{\chi}_1^0$  are the chargino and lowest-mass neutralino states of the minimal supersymmetric standard model (MSSM). For top-squark masses in the range of 180-325 GeV, they simulate both the signal and standard model background processes. Shown in Figure 1 is an example of the signal and background. For this case,  $m_{\tilde{t}_1} = 242$  GeV and  $\lambda'' = 0.03$ .

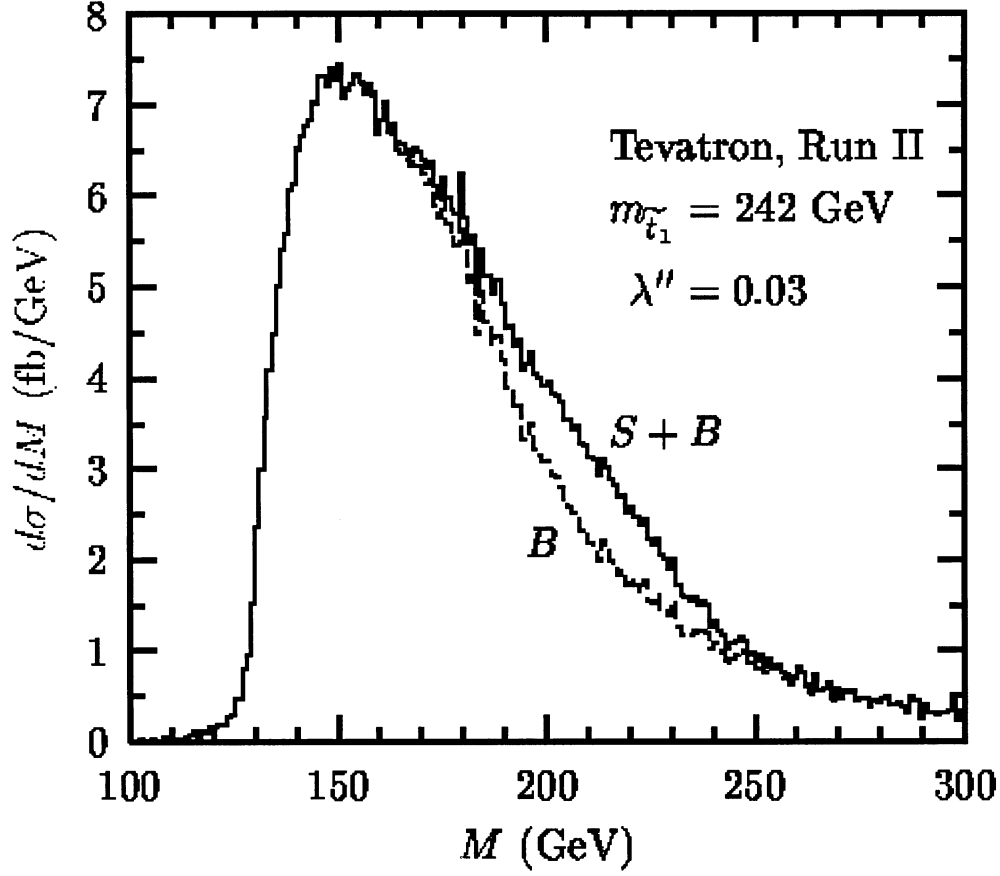


**Figure 1.** The reconstructed-mass  $M$  distribution for single-top-squark production ( $S$ ) and backgrounds ( $B$ ) at the Tevatron ( $\sqrt{S} = 2$  TeV) for a top-squark mass  $m_{\tilde{t}_1} = 242$  GeV. The coupling  $\lambda'' = 0.03$  produces the minimum signal for a  $5\sigma$  significance at this mass.

Figure 2 shows the reach in  $\lambda''$  for  $180 < m_{\tilde{t}_1} < 325$  GeV. With an integrated luminosity of  $2fb^{-1}$  at  $\sqrt{S} = 2$  TeV, discovery at the level of  $5\sigma$  is possible provided that  $\lambda'' > 0.02-0.05$ . Otherwise, a 95% confidence level exclusion can be set for  $\lambda'' > 0.01-0.03$ . By contrast, conventional searches for top squarks via their pair production are limited to masses below 175 GeV. For the lower integrated luminosity and energy of the existing Run I data, values of  $\lambda'' > 0.03-0.2$  can be excluded at the 95% confidence level if  $m_{\tilde{t}_1} = 180-285$  GeV.

Berger, Harris, and Sullivan conclude that, as long as the  $R_p$ -conserving decay  $\tilde{t}_1 \rightarrow b \tilde{\chi}_1^+ \rightarrow Iv \tilde{\chi}_1^0$  is allowed, it should be possible to discover the top squark or to reduce the lower limit on  $\lambda''$  by two orders of magnitude at Run II of the Fermilab Tevatron, for  $180 < m_{\tilde{t}_1} < 325$  GeV and  $\lambda_{3ij}'' > 0.02-0.05$ . Existing data from Run I of the Tevatron should allow a reduction of the limit on  $\lambda''$  by an order of magnitude. With such a reduction, one can establish that  $R_p$ -violating decay is unlikely and rule out most of the possible influence of the top squark on single-top-quark production and decay.

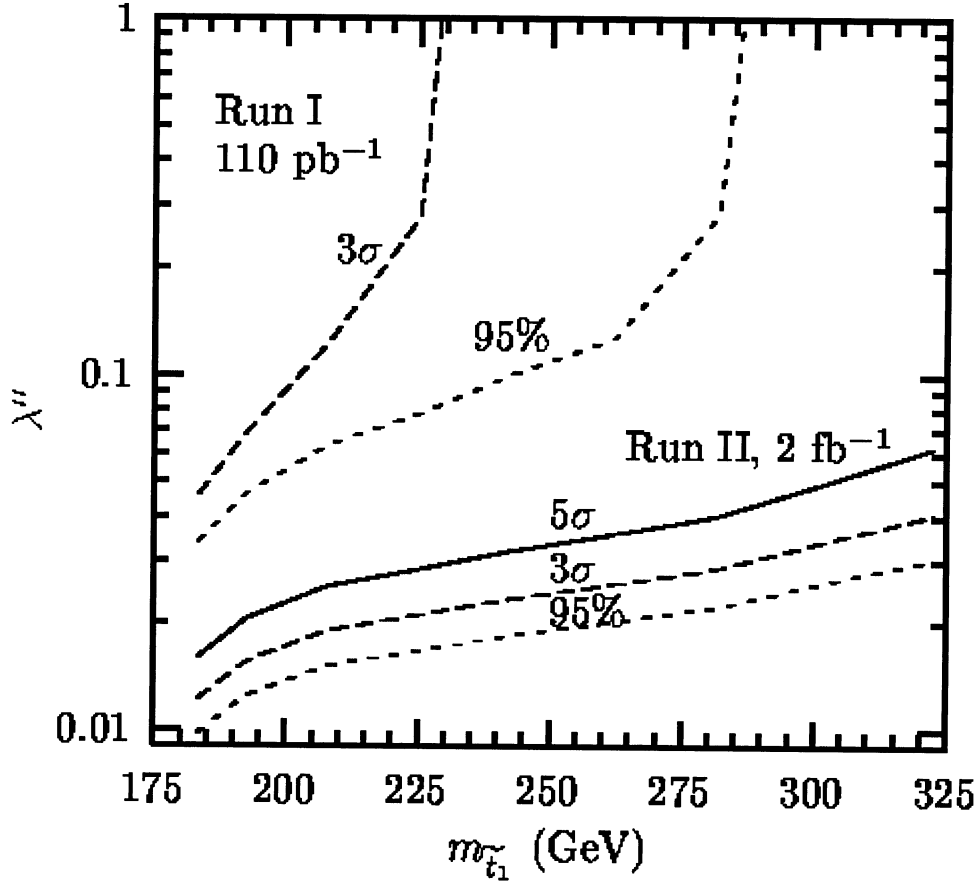


**Figure 2.** Lower limits on discovery ( $S/\sqrt{B} = 5$ ), evidence ( $S/\sqrt{B} = 3$ ), and 95% confidence-level exclusion ( $S/\sqrt{B} = 1.96$ ) for  $\lambda''$  versus top-squark mass in Run I of the Tevatron ( $\sqrt{S} = 1.8$  TeV,  $110\text{pb}^{-1}$ ), and in Run II ( $\sqrt{S} = 2$  TeV,  $2\text{fb}^{-1}$ ).

More research has been done, and a longer paper is in preparation.

(E. L. Berger)

## II.A.2 Resummation of Large Corrections to Heavy-Quarkonium Decays

G. Bodwin and Y.-Q. Chen (ITP, Beijing) have completed a new calculation of the ratio of heavy-quarkonium decay rates  $R = \Gamma(\eta_c \rightarrow \text{light hadrons}) / \Gamma(\eta_c \rightarrow \gamma\gamma)$ . At leading order in the heavy-quark-antiquark velocity  $v$ , this ratio is independent of the nonperturbative heavy-quarkonium matrix elements. Hence, as was shown in a previous paper by Bodwin and Chen [Phys. Rev. **D60**, 054008 (1999)], its perturbation series contains no renormalon ambiguities. Such renormalon ambiguities would be associated with factorial growth of the

terms in the series. In spite of absence of renormalons, the one-loop correction to the ratio  $R$  is large ( $\approx 14.5 \alpha_s / \pi$ ), and the result is very sensitive to the choice of the renormalization scale. Bodwin and Chen noticed that most of the large one-loop correction is proportional to  $\beta_0$ . That is, it comes from vacuum-polarization corrections to the final-state gluon lines in the process  $\eta_c \rightarrow$  light hadrons. This suggests that the large one-loop correction can be brought under control by resumming the vacuum-polarization corrections to all orders.

Bodwin and Chen carried out such a resummation, making use of the method of “naive non-Abelianization” to identify a well-defined, gauge-invariant vacuum-polarization contribution. In this method, one computes the quark-loop contributions to the vacuum polarization, which are well defined, and then replaces  $\beta_0$  the quarks with the full QCD  $\beta_0$  to obtain the effects of gluons. Bodwin and Chen also worked out the resummation for the case of the background-field-gauge vacuum polarization and obtained similar numerical results.

The resumed result depends on the choice of renormalization scale only at the two-loop level, and, so, it is much less sensitive to that choice than is the one-loop result. Therefore, the resummation procedure allows one to make a meaningful comparison between theory and experiment. The agreement is good. In contrast, the result that one obtains by setting the renormalization scale according to the Brodsky-Lepage-Mackenzie (BLM) method overshoots experiment by a factor of five.

The perturbation series that is summed in this method is convergent. Nevertheless, a novel ambiguity arises in the perturbation expression. The answer depends on whether one carries out the final-state phase-space integration first or sums the perturbation series first. This ambiguity can be traced to the regions of the phase-space integration in which a gluon has small virtuality  $q^2$ . In those regions, one does not expect the perturbation series to be reliable. However, Bodwin and Chen have shown that, at any finite order in perturbation theory, one can deform the contour of integration in the complex  $q^2$  plane so that it lies outside of the dangerous region of small  $q^2$ . Therefore, the integrated perturbation expression, in contrast with the differential expression, is reliable in any arbitrarily large, but finite, order in perturbation theory. The conclusion is that the correct procedure is to carry out the phase-space integration first and then sum the perturbation series.

A paper describing this work is in preparation.

(G. T. Bodwin)

### II.A.3 NLO QCD Predictions for SUSY Particle, Jet, and Lepton Pair Production

The discovery or exclusion of supersymmetric (SUSY) particles at hadron colliders depends strongly on solid theoretical cross section predictions in next-to-leading order (NLO) of quantum chromodynamics (QCD). Two calculations of NLO SUSY-QCD cross sections have recently been completed.

The associated production of a chargino/neutralino and a gluino has a potentially large cross section due to the presence of a strong interaction vertex and a potentially light chargino/neutralino and/or gluino. The experimental signature of leptons, jets, and missing energy should be well accessible.

The second channel for which the calculation of the NLO SUSY-QCD cross section was recently completed involves the pair production of charginos/neutralinos and sleptons. It contains two potentially light SUSY particles and in addition has the so-called gold-plated trilepton signature, which should clearly signal the presence of physics beyond the Standard Model.

Furthermore, the status of NLO calculations for hadroproduction of SUSY particles has been reviewed.

Seizing the opportunity of both authors being at the same institution, two NLO QCD programs for jet photoproduction were compared in detail. Very good agreement was found, thus strengthening the basis for comparisons between the theoretical predictions and experimental data.

Like prompt photon production, low-mass lepton pair production in hadron collisions at large transverse momentum can serve to extract the gluon densities in the proton. It has the additional advantage of having no fragmentation contributions and no necessity to isolate the photon. Building on previous work, predictions for a wide variety of possible gluon densities were calculated with the result that fixed target experiments at Fermilab should have good sensitivity to the gluon structure.

(M. Klasen)

## II.A.4 Computational Physics

With the commissioning of RHIC due very soon, our efforts have been concentrated on projects aimed at understanding what QCD predicts for hadronic/nuclear matter at high temperatures and/or baryon number densities, because such an environment is expected to be produced in relativistic heavy ion collisions. In particular, one might hope to see transitions to new states of matter, such as the quark-gluon plasma or one with diquark condensates. For these studies, we are performing simulations in lattice QCD and model field theories.

For hadronic matter at non-zero baryon number density (chemical potential), the fermion determinant of QCD becomes complex and current simulation methods fail. Thus, we have turned to the study of simpler field theories having some of the properties of QCD, which we can simulate with non-zero fermion number density. In particular, we are performing simulations of a 2-colour version of QCD in order to study the formation of diquark condensates in a confining theory. Such condensates have been suggested for QCD at finite quark number density, where they would spontaneously break colour symmetry leading to “colour superconductivity”. Our preliminary simulations of this 2-colour theory show evidence for diquark condensates (Figure 1). We are performing further simulations to map the phase diagram for this theory and to study its phase transitions. In addition, we will measure its spectrum of goldstone bosons, which serve to classify the various phases.

At zero baryon number density, we have been performing simulations of lattice QCD to better understand the finite temperature (chiral) transition from hadronic matter to a quark-gluon plasma. For these simulations we have used a new lattice action for QCD, which includes an irrelevant chiral 4-fermion interaction. This allows us to simulate with zero mass quarks, where this transition becomes a second order phase transition and, in particular, to measure the critical indices at this transition, which allow one to construct the equation of state of hadronic matter near this transition. These simulations are nearing completion and should allow us to determine the universality class of this transition.

Finally, we have been testing a new scheme for lattice quarks -- domain-wall fermions -- that have better chiral properties than standard schemes. In particular, we have been testing how well they approximate the Atiyah-Singer index theorem in the dilute instanton gas, which is high temperature lattice QCD. Related to this, we are checking that the high temperature scalar and pseudoscalar meson excitations have the expected contributions from the zero-modes of the Dirac operator associated with instantons. In particular, we see that these modes alone give rise to the disconnected parts of these propagators, which distinguish flavour singlet mesons from flavour non-singlet mesons. We are now moving to lower temperatures,

where the situation is far less clear and near-zero modes probably start to play a more important rôle.

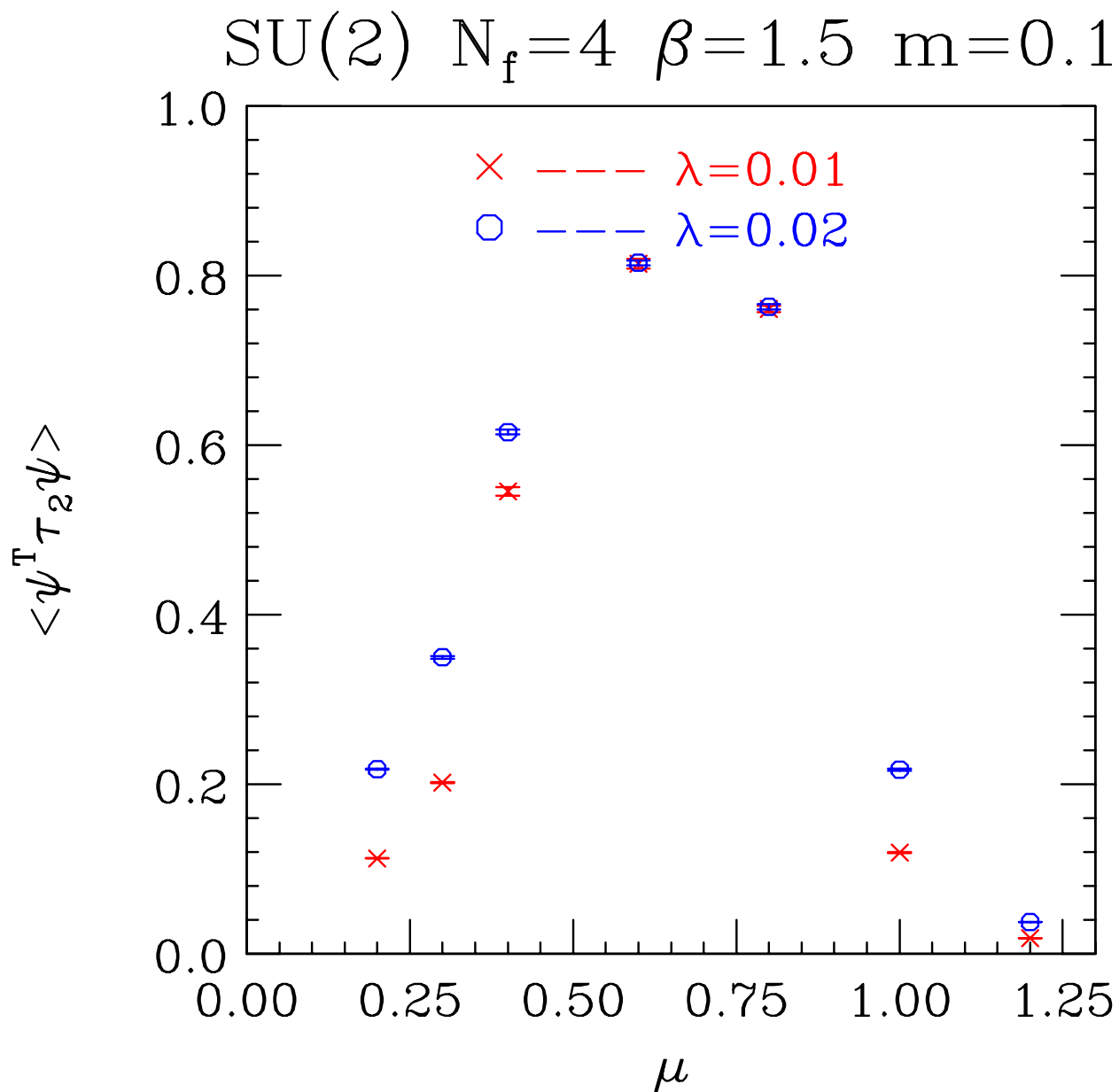


**Figure 1.** Diquark condensate as a function of chemical potential  $\mu$  for quark number.

Our simulations have been performed on supercomputers at NERSC and divisional PCs and workstations.

(D. K. Sinclair)

## II.A.5 Phase-Space Quantization of Field Theory

In prior joint work [J. Phys. **A32**, 771 (1999)], T. Curtright (U. Miami) and C. Zachos have introduced a third, logically independent and complete, formulation of (scalar) quantum field theory, beyond the conventional canonical or path integral quantizations. It is based on quantization in infinite-dimensional field phase-space, which relies on Wigner functions. Wigner's phase-space distribution functions constitute a special representation of the density matrix. The crucial element of this formulation is the interaction picture underlain by the remarkably simple time evolution of the Simple Harmonic Oscillator (rigid classical rotation in phase-space for all quantum configurations, not merely coherent states). See Figure 1.

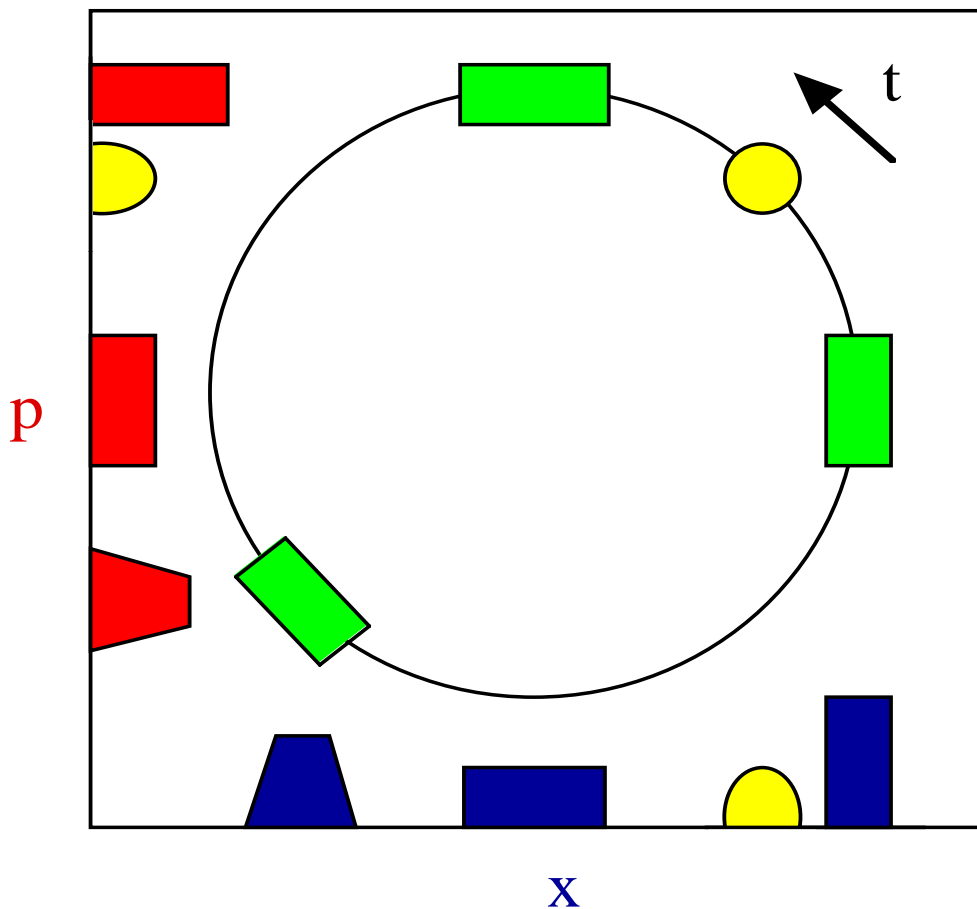


**Figure 1.** Time evolution of arbitrary quantum oscillator configurations.

Quantum fields propagate freely by sitting on an infinity of such uniformly rotating “turntables” and evolve according to merely the interaction part of the hamiltonian in field phase-space.

In pursuit of this longer program, Curtright and Zachos further elucidate how the field dynamics is specified through the evolution of c-number distributions in field phase-space (ANL-HEP-CP-99-06, hep-th/9903254). They moreover utilize canonical transformations to formulate gauge invariance in quantum phase-space, thus deriving the corresponding gauge-invariant Wigner functions from first principles. Finally, they provide a limited discussion of constraints in phase-space, encoded in Dirac brackets.

(C. Zachos)

### **III. ACCELERATOR RESEARCH AND DEVELOPMENT**

#### **III.A. ARGONNE WAKEFIELD ACCELERATOR PROGRAM**

##### **III.A.1 Facility Status/Upgrade Plans**

Work continued on finalizing the design of the new high current photocathode gun. The 1-1/2 cell L-band photocathode RF gun will produce 10 - 100 nC beam with 2-5 ps rms pulse length and normalized emittance less than 100 mm mrad. The final gun design and numerical simulations of the beam dynamics have been completed.

In order to generate high charge and short bunch lengths from a photocathode RF gun, the electric field on the cathode surface has to be very intense. In this way the electrons leaving the cathode surface are quickly accelerated to relativistic velocities, minimizing the bunch lengthening and the emittance growth that the space charge forces produce. There is also bunch lengthening and transverse emittance growth at the exit iris of the gun cavity due to the defocusing forces of the RF fields. Thus, this effect also calls for high accelerating gradient and high beam energy at the exit of the gun. It is therefore desirable to have a multicell gun with high accelerating gradient. Practical considerations (mainly a finite amount of RF power) limit the design to 1-1/2 cells. The choice for our new gun design is a Brookhaven type 1- 1/2 cell cavity scaled up to L band operation. This gun will be followed by one of the present linac tanks that exist at the AWA facility.

A detailed numerical study of this gun was performed with the computer codes SUPERFISH and PARMELA. Table 1 summarizes the parameters used in the simulations. These extensive numerical simulations showed a strong dependence of bunch length and emittance with respect to the accelerating gradient in the gun cavity. Based on these studies, it was decided that an accelerating gradient of 80 MV/m on the cathode surface was a good operating point. This requires 10 MW of RF power to be coupled into the gun cavity, which still leaves enough power to run one of the linac tanks. This accelerating gradient yields good values of emittance and bunch length, while still not high enough to make the RF conditioning of the gun a challenging task. (In fact, we recently conditioned the SRRC gun, a duplicate of the present AWA gun up to a gradient of 125 MV/m.)

**TABLE 1**

**The new photoinjector gun design parameters as calculated using SUPERFISH.**

Inner Radius of the Cell, b (cm)	9.03
Radius of the iris, a (cm)	2.75
Width of the iris, d (cm)	1.5
Aperture of the exit (cm)	2.5
Operating frequency (GHz)	1.3
Initial beam radius (cm)	1
Quality factor, Q	26008
Shunt impedance (MW/m)	36.47

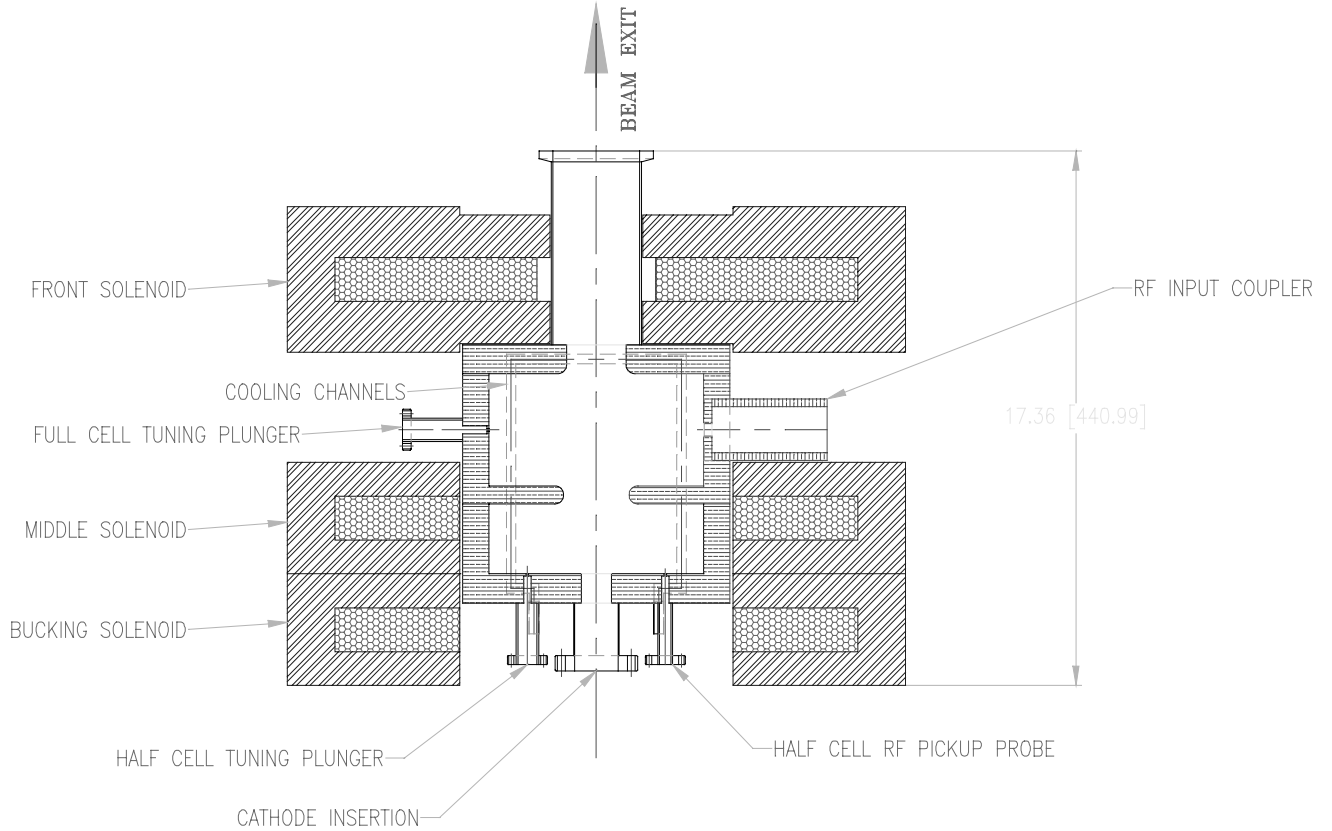


**Figure 1.** Engineering design drawing of the new 1-1/2 cell AWA high current photoinjector.

Figure 1 shows a drawing of the complete photoinjector assembly. Two solenoids are exactly next to each other, with the photocathode plane as their plane of symmetry. This maximizes the space available for the RF power coupler over the full cell of the gun. The tuning plunger in the full cell is located diametrically opposite to the RF coupler, both being at the equator line of the full cell. An RF pickup probe is located half way along the circumference of the full cell between the RF coupler and the tuning plunger. The half cell has both the tuning plunger and the RF pickup probe on the back plate of the cell. This breaks the symmetry of the half cell, but it is acceptable in our L-band size cavity. The perturbation of the field lines over the relatively small size cathode area is negligible. The tuning plungers and RF pickup probes will allow us to verify and, if necessary, to adjust the parameters of the two cells, in order to achieve the right resonance frequency for the pi mode and field balance in the cavity. The cooling channels are drilled along the cylindrical wall of the gun, and also run over part of the back and front plates of the cavity.

The electron beam produced by this gun is expected to excite wakefields in plasmas with accelerating gradients in excess of 1 GeV/m with a plasma density of  $\sim 10^{14}/\text{cm}^3$ . In dielectric loaded structures, this beam will also make a significant improvement over present attainable gradients. One can use this beam to directly demonstrate collinear wakefield acceleration gradients in excess of 50 MV/m corresponding to 200 MW of RF power generated in 30 GHz dielectric structures.

### **III.A.2 Experimental Program**

#### **a. 11.4 GHz Structure**

Work continued on the travelling wave dielectric structure prototype, which we plan to test at SLAC/NLCTA using an X-band klystron rf source. One major challenge in constructing a dielectric loaded travelling wave accelerator powered by an external rf power source is the difficulty in achieving efficient coupling. We have achieved high efficiency broadband coupling by using a combination of a tapered dielectric section and a carefully adjusted coupling slot. We are currently constructing an 11.4 GHz accelerator structure loaded with a permittivity=20 dielectric. Bench testing has demonstrated a coupling efficiency in excess of 95% with bandwidth of 600 MHz. Choice of the dielectric is a MgCaTi compound that has dielectric constant of 20, and is readily obtained from commercial vendors. The group velocity for the NLC design is in the 0.03 c - 0.05c range. The RF coupling scheme used here is similar to the side coupled method used for conventional disk-washer RF cavities. Basically speaking, one would like to obtain maximum RF transmission through the two coupling slots. In order to achieve high efficiency coupling, the dielectric tube near the coupling slots is tapered. The tapered angle was chosen to be 80 for initial convenience. This tapered section serves as a broad band quarter wave transformer for impedance matching. No other angles were tested, but

it is not expected that the taper angle is critical. A 25 cm long prototype structure was constructed.

We plan to continue engineering studies of this accelerating structure with improved RF coupling and mechanical fixture to allow operation in vacuum, eventually leading to a high power test at SLAC of a demonstration accelerator section to resolve practical issues such as breakdown voltage, thermal heating, etc. With 100 MW power, we can test this structure at a 60 MV/m gradient.

#### **b. Multimode Structure Wakefields**

We continued our studies of wakefield excitation and propagation in dielectric structures, particularly concentrating on the case of multiple drive beam excitation in multimode structures. Contrary to recent claims in the literature we have shown that for a collinear multimode structure the amplitude of the wakefield generated by a bunch train is less than or equal to the wakefield generated by a single bunch of the same total charge. Furthermore, the transformer ratio,  $R$ , was shown to be always less than 2, even in the multiple drive beam case. An experiment to measure wakes in a multimode structure at AWA was performed and the results agreed well with our calculations.

A multiple beam, multimode dielectric wakefield accelerator structure was constructed. The structure is a cylindrical dielectric waveguide (permittivity = 38.1) with an inner radius 0.5 cm, outer radius 1.44 cm and 60 cm in length. The AWA can transport a 10 nC beam through a 60 cm long tube with a 1 cm diameter hole. For the multiple beam experiment at AWA, the acceleration wavelength is designed to be 23.05 cm since the rf wavelength is 23.05 cm at 1.3 GHz. Successive drive bunches can then be located one fundamental wavelength apart in the device.

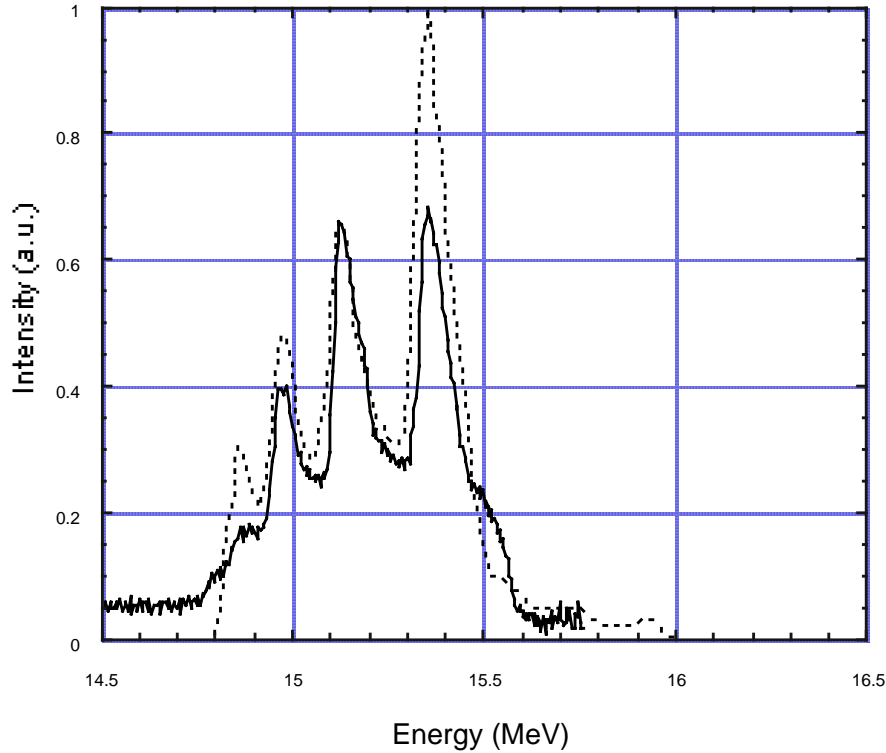


**Figure 2.** Comparison of the predicted (dashed line) and actual (solid line) energy spectrum for the 4 decelerated bunches in the pulse train after passing through the multimode tube. No anomalous transformer ratio enhancement is observed.

Figure 2 shows the calculated and measured spectra for a bunch train of four pulses in the multimode structure. The experimental results are in good agreement with the analytic results: no deviation from conventional linear wakefield theory is observed. This type of wakefield device may still have some utility however. The relatively short rf pulse generated may reduce breakdown and permit higher accelerating gradients to be generated.

### c. Slab Symmetric Laser Driven Accelerators

Advances in the technology of lasers have led to increased interest in their potential applications for accelerating particles. We have proposed a class of resonant dielectric loaded planar structures capable of producing GeV/m accelerating gradients that are driven by laser radiation much as a conventional rf cavity is driven by microwave power from a klystron. The basic idea is the use of a dielectric microstructure, analogous to a Fabry-Perot resonator, consisting of a two parallel dielectric planes separated by a vacuum gap and with a partially transmissive coating on the exterior. Some parameters of the structure are assumed to vary periodically in the beam direction at the wavelength of the illuminating laser. A standing wave with an appropriate phase velocity forward component is induced in this periodic structure by the laser pulse, which in turn accelerates the beam. The laser pulse is swept along the surface of

the structure such that the cavity is filled only in the neighborhood of the beam. The relatively low  $Q$  of these devices (100-1000) and correspondingly short fill times ( $\sim 0.5$  ps) allows gradients of 1 GeV/m to be obtained before breakdown becomes problematic. The beam aspect ratio is highly asymmetric; the ribbon beam-planar structure configuration is advantageous in that dipole deflecting modes are suppressed, analogous to the vanishing of the transverse deflection for  $TM_{0n}$  modes in conventional structures.

Considerable progress has been made in the understanding of slab structure design. We have investigated the use of finite thickness conductive cladding on the structure, with a single coupling slot per period. With this geometry good coupling of laser energy to the accelerating fields can be obtained, while at the same time reducing the surface field/accelerating field ratio significantly over our previous results. The shape of the coupling slot is also seen to be important, in that the introduction of a taper at the slot opening provides improved coupling over the case of a rectangular slot profile.

We analyzed a structure with dielectric thickness ( $b-a$ ) equal to the vacuum gap ( $a = 1.6$  mm), period of 10.6 mm (corresponding to a common CO<sub>2</sub> laser line). The conductive cladding thickness in the simulation is 0.3 mm. The laser coupling and field strengths in the structure were studied as a function of the shape of the coupling slot. While not exhaustive, our calculations indicate a promising approach to the problem of coupling optimization.

Using a tapered 2 mm slot was found to yield a relatively small surface field/gap field ratio (1.56/1.23), while the gap field strength is also a maximum for all similar device geometries.

Resonant planar structures showing good coupling of laser radiation to the desired accelerating mode have been demonstrated numerically, with reasonable surface field/vacuum field strengths and quality factors commensurate with the requirements of a practical accelerator. These properties imply that the structure is a good candidate for further development as an accelerator, as it can be coupled well (it can be fully impedance matched upon filling, just as a standing wave linac cavity). This development will probably proceed at 10.6 micron design wavelength. The choice of this wavelength is based both on availability (e.g. at the UCLA Neptune laboratory), and on mitigation of the experimental challenges one faces on moving orders of magnitude down in accelerator wavelength.

(P.V. Schoessow)

### III.B. MUON COLLIDER R&D

#### III.B.1 Lithium Lens Design

The muon collider operation will depend on the emittance that can be generated by the final cooling element, generally assumed to be a Lithium Lens. This beam emittance generated by the lens is inversely proportional to the current density in the lens, thus this component must be operated near its mechanical limits. In an effort to study the mechanical behavior of the lens and its limits, Ahmed Hassanein of ET has written a code which models the response of the liquid Lithium and its containment vessel using assumed power supply parameters, an equation of state for Lithium from 0 to 1200° C, the penetration of the current into the Lithium and the parameters of the almost cooled muon beam. This was done the HEIGHTS package, which incorporates a self consistent finite element analysis, along with thermal and electromagnetic algorithms. The resistivity of the Lithium is shown in Figure 1, where the operational range is from the melting point, about 180° C, up to about 800° C.

One conclusion of this analysis is that the electrical pulse does not produce a shock, in the normal meaning of the word, since the maximum radial velocity of the 1 cm diameter tube is only 2 m/s. Nevertheless, the beam heating pulse, which momentarily (ns timescales) heats the inner 1 mm of this tube about 500° C, does produce a shock, but one which damps quickly as the energy is distributed through the Lithium.

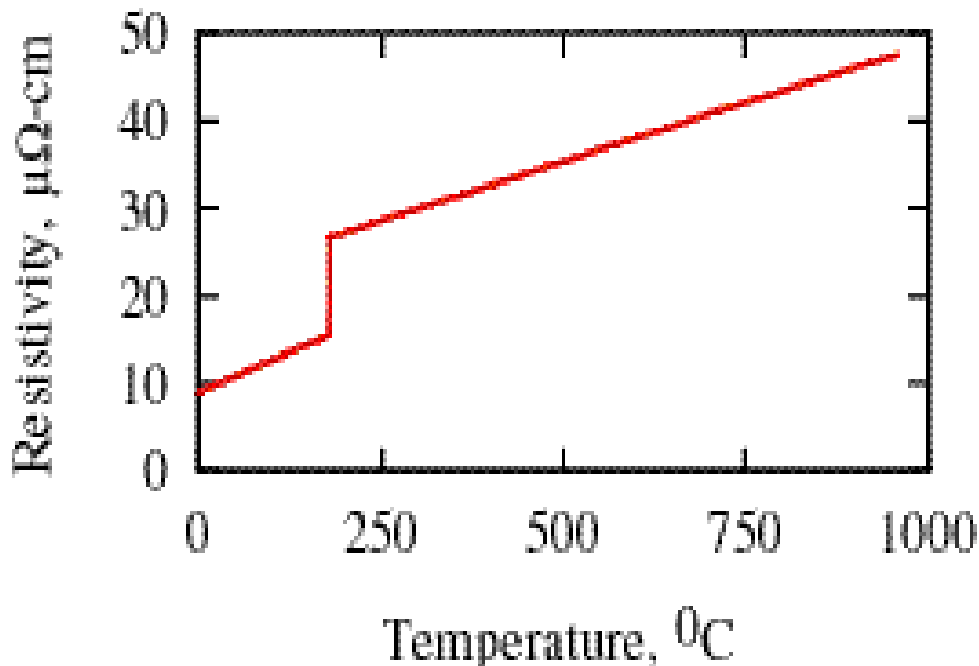


**Figure 1.** The resistivity of Liquid Lithium at high temperatures.

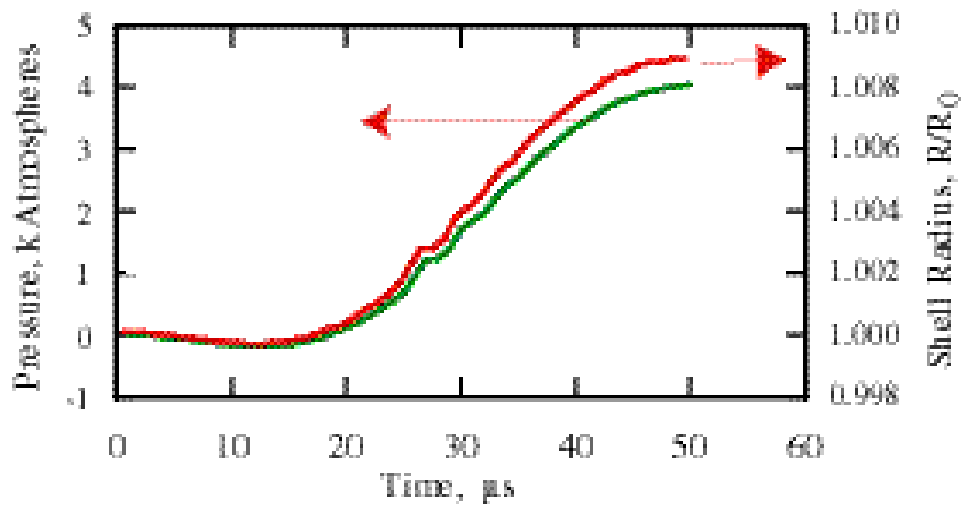


**Figure 2.** The pressure and strain induced by the beam and electrical pulses.

(J. Norem)

## **IV. DIVISIONAL COMPUTING ACTIVITIES**

### **IV.A. GRAND CHALLENGE APPLICATIONS**

#### **IV.A.1 Data Access for High Energy and Nuclear Physics R&D**

Two physicists (L. Price and E. May) and a computer scientist (D. Malon) from DIS division continued to work on the "Grand Challenge Application on HENP Data" project. This is a DOE/ER MICS, HENP-HEP, HENP-NP supported R&D project to provide develop tools to allow High Energy and Nuclear Physicists to analyze and manage the massive amounts of data that will be generated by next generation of experiments. In addition to its direct impact on the success of High Energy and Nuclear Physics experiments this work will also have impact on other governmental and commercial enterprises faced with massive amounts of data. Laboratory and University collaborating partners are LBNL, ANL, BNL, FSU, UCLA, U Tenn., and Yale. For the work in the Atlas-US computing we have been joined in part by two additional physicists (T. LeCompte and R. Wagner).

During this interval we worked in the following areas.

We organized and ran one collaboration meeting at ANL. We participated in the RHIC Mock Data Challenge II at BNL during Feb-Mar using the GCA/HENP data access and storage system to store and analyze STAR and Phenix simulation data. This test was very successful. Guy Pandola (DIS) joined the group to implement the scalability tests that were done at BNL. Interfaces to the CERN "ROOT" analysis system were implemented.

Considerable effort was made on planning the US-Atlas computing organization. A pre-proposal (in collaboration with LBNL) was prepared and submitted to the Atlas-US management to setup and fund an ATLAS-US computing organization. An ANL Assistant Physicist (Tom LeCompte) has joined the group to work on the Atlas related projects. Several visits to CERN were made to give presentations and work with the RD45 and Atlas Database groups. We designed and implemented an extension to the TileCal Testbeam database for offline analysis to be use with and after the July 1999 testbeam runs. We participated in the design and writing of a proposal to DOE for "Next Generation Internet R&D". This work is a natural follow-on and application of the techniques developed "Grand Challenge Application on HENP Data" project. This proposal (The Particle Physics Data Grid) was successful and received funding during FY1999 with the notion of it being a three year project.

(E. N. May)

## V. PUBLICATIONS

### V.A. JOURNAL PUBLICATIONS, CONFERENCE PROCEEDINGS

A 3.9 MeV Photoinjector and Delay System for Wakefield Measurements

J. Power and M. Conde

Rev. Sci. Inst. **69**, 1295 (1998) (*Not previously reported.*)

A High Charge and Short Pulse RF Photocathode Gun for Wakefield Acceleration

W. Gai, X. Li, M. Conde, J. Power, and P. Schoessow

Nucl. Inst. Meth. in Phys. Rev. **A410**, 431 (1998)

(*Not previously reported.*)

A Useful Approximate Isospin Equality for Charmless Strange B Decays

Harry J. Lipkin

Phys. Lett. **B445**, 403-406 (1999)

Analyzing Powers for the  $\pi^- p \rightarrow \pi^0 n$  Reaction Across the  $\Delta$  (1232) Resonance

T.E. Kasprzyk, H.M. Spinka, *et al.*

Phys. Rev. **C60**, 024604 (1999)

Bose-Einstein Correlations and Color Reconnection in W-Pair Production

S.V. Chekanov

Eur. Phys. J. **C6**, 403 (1999)

Bounds on the Lightest Higgs Boson Mass with Three and Four Fermion Generations

D. Dooling, K. Kang, and S. K. Kang

Int. J. Mod. Phys. **A14**, pp. 1605-1632 (1999)

Coherent Multimoded Dielectric Wakefield Accelerators

J. Power, W. Gai and P. Schoessow

Advanced Accelerator Concepts Eighth Workshop,

AIP Conference Proceedings 472, edited by Wes Lawson,

Carol Bellamy, Dorothea F. Brosius (AIP Woodbury, NY, 1999)

p. 686.

Colour-Octet Effects in Radiative Upsilon Decays

F. Maltoni and A. Petrelli

Phys. Rev. **D59**, 074006 (1999)

Coupling Sections, Emittance Growth, and Drift Compensation in the Use of Bent Solenoids as Beam Transport Elements

J. Norem

Phys. Rev. Special Topics - Accelerators and Beams, Vol. 2,

p. 054001 (1999).

Degeneration of ALF  $D_n$  Metrics

G. Chalmers, M. Roček, and S. Wiles  
JHEP **9901**:009 (1999)

Design of a High Charge (10 - 100 nC) and Short Pulse (2 - 5 ps)  
RF Photocathode Gun for Wakefield Acceleration

W. Gai, X. Li, M. Conde, J. Power, and P. Schoessow  
Advanced Accelerator Concepts Eighth Workshop,  
AIP Conference Proceedings 472, edited by Wes Lawson,  
Carol Bellamy, Dorothea F. Brosius (AIP Woodbury, NY, 1999)  
p. 901.

Domain Wall Fermions at Finite Temperature

J.-F. Lagaë and D. K. Sinclair  
Nucl. Phys. Proc. Suppl. **73**:450-452 (1999)

Exclusive Electroproduction of  $\rho^0$  and  $J/\psi$  Mesons at HERA

ZEUS Collaboration, J. Breitweg, *et al.*  
Eur. Phys. J. **C6**, 603 (1999)

Experimental Tests of the Standard Model

L. Nodulman  
Proceedings of the NATO Advanced Study Institute on Techniques  
and Concepts of High Energy Physics X, St. Croix, June 1998,  
edited by T. Ferbel, Kluwer Academic Publishers (1999), pp. 147-  
192.

Forward Jet Production in Deep Inelastic Scattering at HERA

ZEUS Collaboration, J. Breitweg, *et al.*  
Eur. Phys. J. **C6**, 239 (1999)

Higgs-Boson Production in Association with Bottom Quarks at Next-to-Leading  
Order

D. Dicus, T. Stelzer, Z. Sullivan, and S. Willenbrock  
Phys. Rev. **D59**, 094016 (1999)

High Charge Short Electron Bunches for Wakefield Accelerator Structures  
Development

M.E. Conde, W. Gai, R. Konecny, J.G. Power, and P. Schoessow  
Proceedings of the XIX Linac Conference, Vol. 1, edited by  
C.E. Eyberger, R.C. Pardo, and M.M. White  
(ANL-98/28, Argonne, IL, 1999) pp. 100-102.

High Power Test Results of the First SRRC/ANL High Current L-Band RF Gun  
M. Conde, W. Gai, R. Konecny, J. Power, P. Schoessow (ANL), and  
C.H. Ho, *et al.*

Proceedings of the XIX Linac Conference, Vol. 1, edited by  
C.E. Eyberger, R.C. Pardo, and M.M. White  
(ANL-98/28, Argonne, IL, 1999) pp. 520-522.

Improved Staggered Quark Actions with Reduced Flavour Symmetry Violations  
for Lattice QCD

J.-F. Lagaë, D. K. Sinclair, and J. B. Kogut  
Phys. Rev. **D59**, 014511 (1999)

Local Topological and Chiral Properties of QCD

Ph. De Forcrand, M. Garcia Perez, J. E. Hetrick, E. Laermann, J.-F. Lagaë,  
and I.-O. Stamatescu  
Nucl. Phys. Proc. Suppl. **73**:578-580 (1999)

Long-Range Correlations in Deep Inelastic Scattering

S.V. Chekanov  
J. Phys. **G25**, 59 (1999)

Measurement of the  $B_s^0$  Meson Lifetime Using Semileptonic Decays

The CDF Collaboration, F. Abe, *et al.*  
Phys. Rev. **D59**, 032004 (1999)

Measurement of the Diffractive Cross Section in Deep Inelastic Scattering Using  
ZEUS 1994 Data

ZEUS Collaboration, J. Breitweg, *et al.*  
Eur. Phys. J. **C6**, 43 (1999)

Measurement of Jet Shapes in High- $Q^2$  Deep Inelastic Scattering at Hera

ZEUS Collaboration, J. Breitweg, *et al.*  
Eur. Phys. J. **C8**, 367 (1999)

Measurement of Inclusive  $D^* \pm$  and Associated Dijet Cross Sections in  
Photoproduction at HERA

ZEUS Collaboration, J. Breitweg, *et al.*  
Eur. Phys. J. **C6**, 67 (1999)

Measurement of the Top Quark Mass with the Collider Detector at Fermilab

The CDF Collaboration, F. Abe, *et al.*  
Phys. Rev. Lett. **82**, 271 (1999)

Measurement of  $Z^0$  and Drell-Yan Production Cross Section Using Dimuons in  $p\bar{p}$  Collisions at  $\sqrt{s} = 1.8$  TeV

The CDF Collaboration, F. Abe, *et al.*  
Phys. Rev. **D59**, 052002 (1999)

Probing Higgs Bosons with Large Bottom Yukawa Coupling at Hadron Colliders

C. Balázs, J. L. Diaz-Cruz, H.-J. He, T. Tait, and C.-P. Yuan  
Phys. Rev. **D59**, 055016 (1999)

Propagation of Short Electron Pulses in a Plasma Channel

N. Barov, M. Conde, W. Gai, and J.B. Rosenzweig (UCLA)  
Phys. Rev. Lett. **80** (1), 81 (1998) (*Not previously reported.*)

Resonant Excitation of Plasma Wakefields Using Multiple Electron Bunches

Manoel Conde and Wei Gai  
Advanced Accelerator Concepts Eighth Workshop,  
AIP Conference Proceedings 472, edited by Wes Lawson,  
Carol Bellamy, Dorothea F. Brosius (AIP Woodbury, NY, 1999)  
p. 353.

Results From An Iron-Proportional Tube Calorimeter Prototype

P. Schoessow, I. Ambats, D. S. Ayres, J. W. Dawson, W. N. Haberichter,  
N. Hill, R. L. Talaga, and J. L. Thron (ANL), *et al.*  
Proceedings of the VII International Conference on Calorimetry in  
High Energy Physics, edited by Elliott Cheu, Teresa Embry, John  
Rutherford & Richard Wigmans (World Scientific 1998) p. 319.  
(*Not previously reported.*)

RF Power Generation and Coupling Measurements for the Dielectric Wakefield  
Step-Up Transformer

M.E. Conde, W. Gai, R. Konecny, J. Power, P. Schoessow, and P. Zou  
Advanced Accelerator Concepts Eighth Workshop,  
AIP Conference Proceedings 472, edited by Wes Lawson,  
Carol Bellamy, Dorothea F. Brosius (AIP Woodbury, NY, 1999)  
p. 626.

Scale Dependence of Squark and Gluino Production Cross Sections

E. L. Berger, M. Klasen, and T. Tait  
Phys. Rev. **D59**, 074024 (1999)

Scale Invariant Dynamical Fluctuations in Jet Physics

S.V. Chekanov  
Eur. Phys. J. **C6**, 331 (1999)

Solving QCD Via Multi-Regge Theory

A.R. White

Proceedings of the Theory Institute on Deep Inelastic Diffraction,  
Argonne, IL (1998). (*Not previously reported.*)

Spin Structure of the Proton and Large  $p_T$  Processes in Polarized  $pp$  Collisions

L. E. Gordon and G. P. Ramsey

Phys. Rev. **D59**, 074018 (1999)

The Atmospheric Neutrino Flavor Ratio from a 3.9 Fiducial Kiloton Year  
Exposure in Soudan 2

The Soudan 2 Collaboration, W.W. M. Allison, *et al.*

Phys. Lett. **B449**, 137 (1999)

PDK 717

Thermodynamics of Lattice QCD with Massless Quarks and Chiral 4-Fermion  
Interactions

J. B. Kogut, J.-F. Lagaë, and D. K. Sinclair

Nucl. Phys. Proc. Suppl. **73**:471-473 (1999)

Thermodynamics of Lattice QCD with 2 Quark Flavours: Chiral Symmetry and  
Topology

J.-F. Lagaë, D. K. Sinclair, and J. B. Kogut

In: *Adelaide 1998, Nonperturbative Quantum Field Theory*,  
edited by A. W. Schreiber, *et al.* (World Scientific, Singapore,  
1998) pp. 121-131. (*Not previously reported.*)

Three Jet Cross Sections in Photoproduction at HERA

M. Klasen

Eur. Phys. J. **C7**, 225-232 (1999)

Wigner Trajectory Characteristics in Phase Space and Field Theory

T. Curtright and C. Zachos

J. Phys. **A32**, 771-779 (1999)

ZEUS Results on the Measurement and Phenomenology of  $F_2$  at Low  $x$   
and Low  $Q^2$

ZEUS Collaboration, J. Breitweg, *et al.*

Eur. Phys. J. **C7**, 609 (1999)

## V.B. PAPERS SUBMITTED FOR PUBLICATION

Angular Dependence of the  $pp$  Elastic-Scattering Analyzing Power Between 0.8 and 2.8 GeV. I. Results for 1.80 - 2.24 GeV.

C.E. Allgower, D.P. Grossnick, T.E. Kasprzyk, D. Lopiano, H.M. Spinka, *et al.*

Accepted for publication in Phys. Rev. C  
ANL-HEP-PR-99-66

Angular Dependence of the  $pp$  Elastic-Scattering Analyzing Power Between 0.8 and 2.8 GeV. II. Results for Higher Energies

C.E. Allgower, D.P. Grossnick, T.E. Kasprzyk, D. Lopiano, H.M. Spinka, *et al.*

Accepted for publication in Phys. Rev. C  
ANL-HEP-PR-99-67

Associated Production of Gauginos and Gluinos at Hadron Colliders in Next-to-Leading Order SUSY-QCD

E. L. Berger, M. Klasen, and T. Tait

Accepted for publication in Phys. Letts.  
ANL-HEP-PR-99-03

Elastic and Quasi-Elastic  $pp$  Scattering in  ${}^6\text{LiH}$  and  ${}^6\text{LiD}$  Targets Between 1.1 and 2.4 GeV

C.E. Allgower D. Grosnick, T.E. Kasprzyk, D. Lopiano, H.M. Spinka, *et al.*

Accepted for publication in Eur. Phys. J.C.  
ANL-HEP-PR-99-37

Holographic Normal Ordering and Multi-Particle States in the AdS/CFT Correspondence

G. Chalmers and K. Schalm

Nucl. Phys. B  
ANL-HEP-PR-98-143

Measurement of the  $pp$  Analyzing Power in the vicinity of 2.20 GeV

D. Grosnick, D. Lopiano, H.M. Spinka, *et al.*

Eur. Phys. J.C.  
ANL-HEP-PR-99-111

Neutrino Masses, Mixing Angles and the Unification of Couplings in the MSSM

M. Carena, J. Ellis, S. Lola, and C.E.M. Wagner

Nucl. Phys. B  
ANL-HEP-PR-99-76

Observation of a Hybrid Spin Resonance

C. Allgower, H. Spinka, D.G. Underwood, A. Yokosawa, *et al.*

Phys. Rev. Lett.

ANL-HEP-PR-99-75

Quasi-Elastic pn Scattering in  ${}^6\text{LiD}$  and  ${}^6\text{LiH}$  Targets Between 1.1 and 2.4 GeV

C.E. Allgower D. Grosnick, T.E. Kasprzyk, D. Lopiano, H.M. Spinka,  
*et al.*

Accepted for publication in Eur. Phys. J.C.

ANL-HEP-PR-99-38

Search for Nucleon Decay into Lepton +  $\text{K}^0$  Final States Using Soudan 2

D. Wall, for The Soudan 2 Collaboration

Phys Rev. D

ANL-HEP-PR-99-123

PDK-743

Single-Top Squark Production Via R-Parity-Violating Supersymmetric Couplings  
in Hadron Collisions

E. L. Berger, B. W. Harris, and Z. Sullivan

Phys. Rev. Lett.

ANL-HEP-PR-99-05

The Observation of a Shadow of the Moon in the Underground Muon Flux in the  
Soudan 2 Detector

The Soudan 2 Collaboration, J.H. Cobb, *et al.*

Accepted by Phys. Rev. D

ANL-HEP-PR-99-59

PDK-730

The Production of Charginos/Neutralinos and Sleptons at Hadron Colliders

W. Beenakker, M. Klasen, *et al.*

Phys. Rev. Lett.

ANL-HEP-PR-99-71

Wakefield Excitation in Multimode Structures by a Train of Electron Bunches

John G. Power, Wei Gai, and Paul Schoessow

Accepted for publication in Phys. Rev. E

ANL-HEP-PR-99-90

## V.C. PAPERS OR ABSTRACTS CONTRIBUTED TO CONFERENCES

### An ep Collider with $E_{cm} = 1$ TeV in a VLHC Booster Tunnel

M. Derrick, H. Friedrich, A. Gorski, S. Hanuska, J. Jagger, D. Krakauer,  
J. Norem, E. Rotela, S. Sharma, L. Teng, K. Thompson (ANL), T. Sen  
(FNAL), E. Chojnacki (Cornell), D.P. Barber (DESY)  
Proceedings of the 1999 Particle Accelerator Conference  
(PAC '99), New York, NY, March 29 to April 2, 1999.  
ANL-HEP-CP-99-28

### An Optimized Slab-Symmetric Dielectric-Based Laser Accelerator Structure

P.V. Schoessow, and J.B. Rosenzweig  
Proceedings of the 8<sup>th</sup> Workshop on Advanced Accelerator  
Concepts (AAC '98), Baltimore, MD, July 5-11, 1998.  
ANL-HEP-CP-99-104

### Atmospheric Neutrinos in Soudan 2

Maury Goodman, for the Soudan 2 Collaboration  
Proceedings of the Division of Particles and Fields (DPF'99)  
Los Angeles, CA, January 6-9, 1999.  
ANL-HEP-CP-99-8  
PDK-719

### Atmospheric Neutrinos in Soudan 2

Maury Goodman, for The Soudan 2 Collaboration  
Proceedings of the XXVI International Cosmic Ray Conference,  
Salt Lake City, Utah, August 17-25, 1999.  
ANL-HEP-CP-99-63  
PDK-734

### $B_d^0$ Mixing and CP Violation Measurements at the Tevatron

K. L. Byrum  
Proceedings of the 34<sup>th</sup> Rencontres de Moriond, Les Arcs, France,  
March 20-27, 1999.  
ANL-HEP-CP-99-64

### Bent Solenoids for Spectrometers and Emittance Exchange Sections

J. Norem  
Proceedings of the 1999 Particle Accelerator Conference  
(PAC '99) New York, NY, March 29 to April 2, 1999.  
ANL-HEP-CP-99-30

### Construction and Testing of an 11.4 GHz Dielectric Structure Based Travelling Wave Accelerator

P. Zou, W. Gai, R. Konecny, and T. Wong  
Proceedings of the 1999 Particle Accelerator Conference (PAC '99)  
New York, NY, March 29 to April 2, 1999.  
ANL-HEP-CP-99-31

Cosmic Ray Sun Shadow in Soudan 2 Underground Muon Flux

The Soudan 2 Collaboration, W.W.M. Allison, *et al.*

Proceedings of the XXVI International Cosmic Ray Conference,  
Salt Lake City, Utah, August 17-25, 1999.

ANL-HEP-CP-99-60

PDK-731

CTEQ5 Parton Distributions and Ongoing Studies

S. Kuhlmann

Proceedings of the 7<sup>th</sup> International Workshop on Deep Inelastic  
Scattering and QCD, Zeuthen, Germany, April 19-23, 1999.

ANL-HEP-CP-99-95

Cygnus X-3 Revisited: 10 Years of Muon and Radio Observations

The Soudan 2 Collaboration, W.W.M. Allison, *et al.*

Proceedings of the XXVI International Cosmic Ray Conference,  
Salt Lake City, Utah, August 17-25, 1999.

ANL-HEP-CP-99-61

PDK-732

Design and Construction of a High Charge and High Current 1-1/2 Cell L-Band  
RF Photocathode Gun

M.E. Conde, W. Gai, R. Konecny, J.G. Power, and P. Schoessow

Proceedings of the 1999 Particle Accelerator Conference (PAC '99)  
New York, NY, March 29 to April 2, 1999.

ANL-HEP-CP-99-26

Detailed Comparison of Next-to-Leading Order Predictions for Jet Photoproduction  
at HERA

B. W. Harris, M. Klasen, and J. Vossebeld

DESY Workshop on Monte Carlo Generators for HERA Physics,  
Hamburg, Germany, February 1-5, 1999.

ANL-HEP-CP-99-43

Heavy Quark Production in Deep-Inelastic Scattering at HERA

B. W. Harris, E. Laenen, S. Moch, and J. Smith

DESY Workshop on Monte Carlo Generators for HERA Physics,  
Hamburg, Germany, February 1-5, 1999.

ANL-HEP-CP-99-35

Low Mass Lepton Pair Production in Hadron Collisions

E. L. Berger and M. Klasen

International Conference on the Structure and Interactions of the  
Photon (PHOTON '99), Freiburg, Germany, May 23-27, 1999.

ANL-HEP-CP-99-72

Neutrino Induced Muons in Soudan 2

D.M. DeMuth, for The Soudan 2 Collaboration

Proceedings of the XXVI International Cosmic Ray Conference,  
Salt Lake City, UT, August 17-25, 1999.

ANL-HEP-CP-99-57

PDK-728

Nucleon Decay in Soudan 2

M.C. Goodman, for The Soudan 2 Collaboration

Proceedings of the XXVI International Cosmic Ray Conference,  
Salt Lake City, Utah, August 17-25, 1999.

ANL-HEP-CP-99-56

PDK-727

Observation of the Moon Shadow in Deep Underground Muon Flux

The Soudan 2 Collaboration, J. H. Cobb, *et al.*

Proceedings of the XXVI International Cosmic Ray Conference,  
Salt Lake City, Utah, August 17-25, 1999.

ANL-HEP-CP-99-58

PDK-729

Phase-Space Quantization of Field Theory

C. Zachos and T. Curtright

Workshop on Gauge Theory and Integrable Models, Kyoto, Japan,  
January 26-29, 1999.

ANL-HEP-CP-99-06

R-Parity-Violating Production of Single Top Squarks with R-Parity-Conserving Decays

E. L. Berger, B. W. Harris, and Z. Sullivan

XXXIV Recontres de Moriond on QCD and High Energy and  
Hadronic Interactions, Les Arcs, Savoie, France, March 20-27,  
1999.

ANL-HEP-CP-99-42

Search for Neutrinos from Active Galactic Nuclei in Soudan 2

D.M. DeMuth, for The Soudan 2 Collaboration

Proceedings of the XXVI International Cosmic Ray Conference,  
Salt Lake City, UT, August 17-25, 1999.

ANL-HEP-CP-99-55

Searching for R-Parity Violation at Run-II of the Tevatron

E. L. Berger, B. W. Harris, and Z. Sullivan, *et al.*

Workshop on Physics at Run II: Supersymmetry/Higgs, Batavia,  
IL, November 19-21, 1998.

ANL-HEP-CP-99-74

Seasonal Variations in Soudan 2

M.C. Goodman, for The Soudan 2 Collaboration

Proceedings of the XXVI International Cosmic Ray Conference,  
Salt Lake City, Utah, August 17-25, 1999.

ANL-HEP-CP-99-62

PDK-733

Short-Bunch Production and Microwave Instability Near Transition

J. Norem and K.Y. Ng

Proceedings of the Workshop on Stabilities of Intense Hadron  
Beams in Rings, Upton, NY, June 28-July 1, 1999.

ANL-HEP-CP-99-100

Single-Top-Squark Production Via Baryon-Number Violating Couplings at the  
Fermilab Tevatron Collider

E. L. Berger, B. W. Harris, and Z. Sullivan

Workshop on Physics at Run II: Supersymmetry/Higgs, Batavia,  
IL, November 19-21, 1998.

ANL-HEP-CP-99-40

Slab Symmetric Dielectric Micron Scale Structures for High Gradient Electron  
Acceleration

P.V. Schoessow, and J.B. Rosenzweig

Proceedings of the 1999 Particle Accelerator Conference (PAC '99)  
New York, NY, March 29 to April 2, 1999.

ANL-HEP-CP-99-65

Status of the New Muon (g-2) Experiment

L. Nodulman and the Muon (g-2) Collaboration

Proceedings 17<sup>th</sup> International Workshop on Weak Interactions and  
Neutrinos (WIN99), Cape Town, South Africa, January 1999, 5p.

ANL-HEP-CP-99-41

Studies of Slow-Positron Production Using Low-Energy Primary Electron Beams

E. Lessner, D. Mangra, J.G. Power, P. Schoessow, and M. White

Proceedings of the 1999 Particle Accelerator Conference  
(PAC'99),

New York, NY, March 29 to April 2, 1999.

ANL-HEP-CP-99-46

Summary of Experimental Electroweak Physics

L. Nodulman

Proceedings 17<sup>th</sup> International Workshop on Weak Interactions and  
Neutrinos (WIN99), Cape Town, South Africa, January 1999, 7p.

hep-ex/9904012

ANL-HEP-CP-99-33

Tevatron Direct Photon Results

S. Kuhlmann

Proceedings of the 7<sup>th</sup> International Workshop on Deep Inelastic Scattering and QCD, Zeuthen, Germany, April 19-23, 1999.  
ANL-HEP-CP-99-96

The Design of a Liquid Lithium Lens for a Muon Collider

A. Hassanein, J. Norem, C. Reed (ANL), and R. Palmer, et al.

Proceedings of the 1999 Particle Accelerator Conference (PAC '99)  
New York, NY, March 29 to April 2, 1999.  
ANL-HEP-CP-99-29

The FEL Development at the Advanced Photon Source

S.V. Milton, N.D. Arnold, C. Benson, S. Berg, and J. Power, *et al.*

Free-Electron Laser Challenges II, part of SPIE's Photonics West '99,  
San Jose, CA, January 23-29, 1999.  
SPIE paper #3614 16

Updated Calculations of the Reach of Fermilab Tevatron Upgrades for Higgs Bosons in the MSSM, mSUGRA, and mGMSB Models

H. Baer, B. W. Harris, and X. Tata

Workshop on Physics at Run II: Supersymmetry/Higgs, Batavia, IL, November 19-21, 1998.  
ANL-HEP-CP-99-34

Wakefield Excitation in Multimode Structures by a Train of Electron Bunches

M.E. Conde, W. Gai, R. Konecny, and P. Schoessow

Proceedings of the 1999 Particle Accelerator Conference (PAC '99)  
New York, NY, March 29 to April 2, 1999.  
ANL-HEP-CP-99-27

**V.D. TECHNICAL REPORTS AND NOTES**

Master Plate Production for the Tile Calorimeter Extended Barrel Modules

J. Proudfoot, V. Guarino, K. Wood, N. Hill, E. Petereit, and L. Price  
ANL-HEP-TR-99-04

$\chi^2$  and Correlated Systematic Errors

G. T. Bodwin and E. Kovacs  
CDF Note, CDF/ANAL/JET/CDFR/5005

**CDF Notes:**

CDF-4839

“Lateral Shower Modification in QFL”

K. Byrum

CDF-4844

“Comparison of the Total Cross Section Measurements of CDF and E-811”

M. Albrow, A. Beretvas, L. Nodulman, P. Giromini (Fermilab-TM-2071).

CDF-4910

“Rub 1b Prompt Cross Section”

D. Partos, S. Kuhlmann, J. Lamoureux,

CDF-4928

“Direct Measurement of  $\Gamma_W$  with Run b 1b Muons”

A. Hardman and A. Garfinkel

CDF-4929

“Backgrounds to the Direct Measurement of  $\Gamma_W$  with Run 1b Muons”

A. Hardman and A. Garfinkel

CDF-4998

“ $B_d^0$  Mixing and CP Violation Measurements at the Tevatron”

K. Byrum

CDF-5001

“Luminosity for Run 1b Inclusive Electron Binary Dataset”

K. Byrum

CDF-5002

“Summary of  $B_c$  Decay to  $J/\psi \pi D_s$ ”

A. B. Wicklund

CDF-5022

“Tevatron Direct Photon Results”

S. Kuhlmann

### MUCOOL Notes:

MuCool Note #21  
Bunched Muons from the FNAL Booster  
Jim Norem  
6/02/99

MuCool Note #29  
A Panofsky Quadrupole for a Low energy FFAG  
Jim Norem  
6/02/99

### NuMI Notes:

NuMI-L-473  
The Hybrid Emulsion Detector for MINOS R&D Proposal (Version 3.0)  
The MINOS Collaboration, P. Adamson, *et al.*

NuMI-L-492  
Seasonal Variations of the Trigger Rate and the Muon Rate in Soudan 2  
W.L. Barrett, M.C. Goodman, D. Jankowski, and W. Miller  
PDK-720

### PDK Notes:

PDK-717  
The Atmospheric Neutrino Flavor Ratio from a 3.9 Fiducial Kiloton Year  
Exposure in Soudan 2  
The Soudan 2 Collaboration, W.W. M. Allison, *et al.*  
Phys. Lett. **B449**, 137 (1999)  
(e-Print Archive: hep-ex/9901024)  
ANL-HEP-PR-99-2

PDK-719  
Atmospheric Neutrinos in Soudan 2  
M. C. Goodman, for The Soudan 2 Collaboration  
ANL-HEP-CP-99-8

PDK-720  
Seasonal Variations of the Trigger Rate and the Muon Rate in Soudan 2  
W. L. Barrett, M. C. Goodman, D. Jankowski, and W. Miller  
NuMI-L-492

- PDK-726  
Search for Neutrinos from Active Galactic Nuclei in Soudan 2  
D.M. DeMuth, for The Soudan 2 Collaboration  
ANL-HEP-CP-99-55
- PDK-727  
Nucleon Decay in Soudan 2  
M.C. Goodman, for The Soudan 2 Collaboration  
ANL-HEP-CP-99-56
- PDK-728  
Neutrino Induced Muons in Soudan 2  
D.M. DeMuth, for The Soudan 2 Collaboration  
ANL-HEP-CP-99-57
- PDK-729  
Observation of the Moon Shadow in Deep Underground Muon Flux  
The Soudan 2 Collaboration, J. H. Cobb, *et al.*  
ANL-HEP-CP-99-58
- PDK-730  
The Observation of a Shadow of the Moon in the Underground Muon Flux  
in the Soudan 2 Detector  
The Soudan 2 Collaboration, J. H. Cobb, *et al.*  
ANL-HEP-PR-99-59
- PDK-731  
Cosmic Ray Sun Shadow in Soudan 2 Underground Muon Flux  
The Soudan 2 Collaboration, W.W.M. Allison, *et al.*  
ANL-HEP-CP-99-60
- PDK-732  
Cygnus X-3 Revisited: 10 Years of Muon and Radio Observations  
The Soudan 2 Collaboration, W.W.M. Allison, *et al.*  
ANL-HEP-CP-99-61
- PDK-733  
Seasonal Variations in Soudan 2  
M.C. Goodman, for the Soudan 2 Collaboration  
ANL-HEP-CP-99-62
- PDK-734  
Atmospheric Neutrinos in Soudan 2  
M.C. Goodman, for The Soudan 2 Collaboration  
ANL-HEP-CP-99-63

**Wakefield Notes:**

WF-183

RF Photoinjector Based Two Beam Accelerator Research Plan at Argonne

Wei Gai

April 15, 1999

WF-184

Summary of June 2 Step-up Transformer Experiment Run

Wei Gai

June 3, 1999

## VI. COLLOQUIA AND CONFERENCE TALKS

### **Edmond L. Berger**

Associated Production of a Gaugino and a Gluino at Hadron Colliders in NLO QCD

DOE Review of High Energy Physics Division, Argonne, IL,  
June 11, 1999.

Cross Sections for Associated Production of a Gluino and a Gaugino at Hadron Colliders in Next-to-leading Order SUSY-QCD

Higgs and Supersymmetry Search and Discovery Conference, University of Florida, Gainesville, FL, March 8-11, 1999.

Open Issues in Prompt Photon Production in Hadron Reactions

Physics at Run II - Workshop on QCD and Weak Boson Physics,  
Batavia, IL, March 4-6, 1999.

Supersymmetric Particle Production at Hadron Colliders in Next-to-Leading Order SUSY-QCD

University of Minnesota, Minneapolis, MN, February 25, 1999.

Supersymmetric Particle Production at Hadron Colliders in Next-to-Leading Order QCD

Aspen Winter Physics Conference, Aspen Center for Physics, Aspen, CO,  
January 19, 1999.

### **Gordon Chalmers**

Holographic Normal Ordering in the AdS/CFT Correspondence

Cargese Summer School 1999, "Progress in String Theory and M-Theory," Cargese, Italy, May 24 – June 5, 1999.

Correlation Functions in the AdS/CFT Correspondence

Durham University, England, May 17-24, 1999.

Correlation Functions, Holographic Normal Ordering and Multi-Particle States in the AdS/CFT Correspondence

SLAC, Stanford, CA, March 3, 1999.

Correlation Functions, Holographic Normal Ordering and Multi-Particle States in the AdS/CFT Correspondence

LBNL, Berkeley, CA, March 1-2, 1999.

Correlation Functions, Holographic Normal Ordering and Multi-Particle States in the AdS/CFT Correspondence  
Caltech, Pasadena, CA, February 25-26, 1999.

Correlation Functions, Holographic Normal Ordering and Multi-Particle States in the AdS/CFT Correspondence  
UCLA, Los Angeles, CA, February 22-26, 1999.

Correlation Functions, Holographic Normal Ordering and Multi-Particle States in the AdS/CFT Correspondence  
ITP, Santa Barbara, CA, February 7-21, 1999.

### **Wei Gai**

Recent Dielectric/Plasma Wakefield Experimental Results at ANL.  
Brookhaven National Lab, Upton, NY, January 19, 1999.

### **Maury Goodman**

Atmospheric Neutrino Results in Soudan 2  
Invited talk, DPF'99 Division of Particles and Fields Conference, UCLA, Los Angeles, CA, January 1999.

Long-Baseline Experiments for a Long Time  
Invited talk, The 23<sup>rd</sup> John Hopkins Workshop on Current Problems in Particle Theory: Neutrinos in the Next Millennium  
John Hopkins University, Baltimore, MD, June 1999.

Our Minnesota Neutrinos Can Beat Your Neutrinos: Results from Soudan 2 and Plans for MINOS  
Physics Colloquium, Louisiana State University, May 7, 1999.

The Neutrino Oscillation Industry  
Physics Colloquium, Purdue University, January 14, 1999.

### **Brian Harris**

Open Heavy-Flavor Production in DIS at NLO  
Invited lecture presented at the Ringberg Workshop on New Trends in HERA Physics, Rottach-Egern, Germany, May 30 – June 4, 1999.

Summary of Higgs and Supersymmetry: Search and Discovery  
ANL-HEP Lunch Seminar, March 23, 1999.

Reach of Fermilab Tevatron Upgrades for Higgs Bosons in Supersymmetric Models

Higgs and Supersymmetry Search and Discovery Conference, University of Florida, Gainesville, FL, March 8-11, 1999.

Updated Calculations of the Reach of Fermilab Tevatron Upgrades for SUSY Higgs Bosons

Higgs Working Group Meeting, FNAL, Batavia, IL, January 29, 1999.

### **Michael Klasen**

Low Mass Lepton Pair Production in Hadron Collisions

Workshop on Physics at Run II -- QCD and Weak Boson Physics, Fermilab, Batavia, IL, June 3-4, 1999.

Photon Structure and the Production of Jets, Hadrons, and Photons

Invited lecture presented at the Ringberg Workshop on New Trends in HERA Physics, Rottach-Egern, Germany, May 30 – June 4, 1999.

Low Mass Lepton Pair Production in Hadron Collisions

International Conference on the Structure and Interactions of the Photon (PHOTON '99), Freiburg, Germany, May 23-27, 1999.

Gaugino Production at Hadron Colliders in NLO QCD

Physics Department, Indiana University, Bloomington, April 19, 1999.

Gaugino Production at Hadron Colliders in NLO QCD

PHENO '99 Symposium, Phenomenology for the Third Millennium, University of Wisconsin, Madison, April 12, 1999.

Gaugino Production at Hadron Colliders in NLO QCD

ANL-HEP Theoretical Physics Seminar, March 15, 1999.

Low Mass Lepton Pair Production in Hadron Collisions

Michigan State University, East Lansing, MI, February 24, 1999.

A NLO MC Generator for the Photoproduction of Jets at HERA

DESY Workshop on Monte Carlo Generators for HERA Physics, Hamburg, Germany, February 1-5, 1999.

Gaugino Production at Hadron Colliders in NLO QCD

Technical University, Munich Germany, January 27-31, 1999.

Gaugino Production at Hadron Colliders

Division of Particles and Fields Conference (DPF '99), Los Angeles, CA, January 5-9, 1999.

**Harry J. Lipkin**

Bose-Einstein Correlation for “Almost Identical” Particles  
University of California, Irvine, March 11, 1999.

**Lawrence J. Nodulman**

CP Violation in B Decay at CDF  
University of Texas, Austin, Texas, March 1999.

CP Violation in B Decay at CDF  
University of Utah, Salt Lake City, Utah, April 1999.

Measuring the W Mass with the Upgrade  
Precision Subgroup, Run II QCD and Weak Boson Physics Workshop,  
Fermilab, March 1999.

**Donald K. Sinclair**

High Temperature Meson Propagators with Domain-Wall Quarks  
XVII International Symposium on Lattice Field Theory (LATTICE '99),  
Pisa, Italy, June 28 – July 3, 1999.

**Hal Spinka**

Notes on the RHIC Polarimeter  
RHIC Spin Working Group, Brookhaven National Laboratory, May 1999.

**Zack Sullivan**

R-Parity Violation and Single Top Squarks at the Tevatron  
Fermilab, Batavia, IL, May 6, 1999.

R-Parity-Violating Production of Single Top-Squarks with R-Parity-Conserving  
Decays  
PHENO '99 Symposium, Phenomenology for the Third Millennium,  
University of Wisconsin, Madison, April 13, 1999.

A Summary of Moriond: QCD and High Energy Interactions  
ANL-HEP Lunch Seminar, April 6, 1999.

R-Parity-Violating Production of Single Top-Squarks with R-Parity-Conserving Decays

XXXIV Recontres de Moriond on QCD and High Energy and Hadronic Interactions, Les Arcs, Savoie, France, March 26, 1999.

R-Parity-Violating Production of Single Top-Squarks with R-Parity-Conserving Decays

Higgs and Supersymmetry Search and Discovery Conference, University of Florida, Gainesville, FL, March 8, 1999.

### **Timothy Tait**

Associated Production of a Gluino with a Gaugino at Hadron Colliders in NLO QCD

7<sup>th</sup> International Conference on Supersymmetries in Physics (SUSY '99), Batavia, IL, June 14-19, 1999.

### **Carlos Wagner**

On Higgs Searches at the LEP and the Tevatron Colliders

1999 Summer Workshop on Phenomenology of Super Particles and Super Branes, Aspen, CO, June 28-July 12, 1999.

The Complementarity of LEP, the Tevatron and the LHC in the Search for a Light MSSM Higgs Boson

7<sup>th</sup> International Conference on Supersymmetries in Physics (SUSY '99), Batavia, IL, June 14-19, 1999.

### **Cosmas Zachos**

The Wigner Phase-Space Quasi-Probability Distribution Function

Department of Physics, Ohio State University, Columbus, May 26, 1999.

Quantum Mechanics Lives and Works in Phase Space

ANL Physics Division Colloquium, February 19, 1999.

Phase-Space Quantization of Field Theory

Workshop on Gauge Theory and Integrable Models, Yukawa Institute of Theoretical Physics, Kyoto, Japan, January 29, 1999.

## VII. HIGH ENERGY PHYSICS COMMUNITY ACTIVITIES

### **David S. Ayres**

MINOS Project Manager, Acting.

Deputy Spokesperson for the MINOS Collaboration.

### **Edmond L. Berger**

Adjunct Professor of Physics, Michigan State University, East Lansing, MI,  
1997-present.

Member, High Energy and Nuclear Physics Advisory Committee, Brookhaven  
National Laboratory, 1995-2001.

Chair, Subgroup on SUSY Production Cross Sections, Fermilab Workshop on  
Physics at Run II -- Supersymmetry/Higgs, Batavia, IL, November 19-21,  
1998.

Convenor, Physics at Run II Working Group on Photons and Weak Bosons,  
Fermilab, Batavia, IL, January - December, 1999.

Member, Scientific Program Committee, Recontres de Moriond, QCD and High  
Energy Hadronic Interactions, Les Arcs, France, March 1998 and March  
1999.

Organizing Committee, Seventh Conference on the Intersections Between Particle  
and Nuclear Physics, May-June, 2000.

Member, Local Organizing Committee, International Conference on Kaon  
Physics (K'99), University of Chicago, Chicago, IL, June 21-26, 1999.

Member, International Advisory Committee, Eighth International Conference on  
Hadron Spectroscopy, Beijing, China, August, 1999.

Member, International Advisory Committee, Frontiers in Science '99, Blois,  
France, June-July, 1999.

**Wei Gai**

Member, Advanced Accelerator Workshop Scientific and Organizing Committee.

**Maury C. Goodman**

Member, MINOS Executive Committee.

Member, Particle Data Group.

**Michael Klasen**

Member, Program Committee, International Conference on the Structure and Interactions of the Photon (PHOTON '99), Freiburg, Germany, May 23-27, 1999.

**Harry J. Lipkin**

Member, International Advisory Committee, Eighth International Conference on Hadron Spectroscopy, Beijing, China, August, 1999.

**Edward N. May**

Member, Staff of ESnet Steering Committee.

**Lawrence J. Nodulman**

Co-Electroweak Organizer (with P. Langacker), 17<sup>th</sup> International Workshop on Weak Interactions and Neutrinos (WIN99), Cape Town, South Africa, January 1999.

**James Norem**

Muon Collider Group, Technical Committee.

**Lawrence E. Price**

Chair, ESnet Steering Committee.

**Jose Repond**

Member, International Advisory Committee for workshop series, "Deep Inelastic Scattering and QCD," Berlin, Germany, 1999; and Liverpool, Great Britain, 2000.

**Hal Spinka**

Chairman - Technical, Cost, and Schedule review for the Los Alamos  $n + p \rightarrow d + \gamma$  experiment.

**Alan R. White**

Member, Program Committee, XXIXth International Symposium on Multiparticle Dynamics, Brown University, Providence, RI, August, 1999.

## VIII. HEP DIVISION RESEARCH PERSONNEL

### Administration

L. Price

D. Hill

### Accelerator Physicists

M. Conde

J. Power

W. Gai

P. Schoessow

J. Norem

### Experimental Physicists

D. Ayres

B. Musgrave

R. Blair

L. Nodulman

K. Byrum

J. Proudfoot

S. Chekanov

J. Repond

M. Derrick

H. Spinka

T. Fields

R. Stanek

M. Goodman

R. Talaga

D. Krakauer

J. Thron

S. Kuhlmann

R. Thurman-Keup

T. LeCompte

D. Underwood

T. Joffe-Minor

R. Wagner

S. Magill

A. Wicklund

E. May

A. Yokosawa

R. Yoshida

### Theoretical Physicists

E. Berger

D. Sinclair

G. Bodwin

Z. Sullivan

G. Chalmers

T. Tait

B. Harris

C. Wagner

M. Klasen

A. White

J. -F. Lagaë

C. Zachos

A. Petrelli

### Engineers, Computer Scientists, and Applied Scientists

J. Dawson

N. Hill

G. Drake

E. Kovacs

V. Guarino

J. Schlereth

W. Haberichter

X. Yang

### **Technical Support Staff**

I. Ambats  
A. Caird  
G. Cox  
D. Jankowski  
T. Kasprzyk  
C. Keyser  
L. Kocenko

R. Konecny  
Z. Matijas  
E. Petereit  
L. Reed  
R. Rezmer  
R. Taylor  
K. Wood

### **Laboratory Graduate Participants**

C. Allgower  
J. Breitweg  
A. Hardman

D. Mikunas  
H. Zhang  
P. Zou

### **Visiting Scientists**

Y.-C. Chen (Theory)  
E. Kovacs (Theory)  
H. Lipkin (Theory)  
P. Orland (Theory)

G. Ramsey (Theory)  
J. Uretsky (Theory)  
T. Wong (AWA)  
Sun, Xiang (AWA)